Project Number: MQP-DEH-UMA3

Surface Derivatization of Glucan Particles for Drug Delivery

A Major Qualifying Project

Submitted to the Faculty
Of the
WORCESTER POLYTECHNIC INSTITUTE

In Partial Fulfillment of the Requirements for the
Degree of Bachelor of Science

By:

_____
Melissa K. Castle

Date: April 28, 2011

Approved:

_____
Professor Destin Heilman, Advisor

Abstract

Glucan particles (GPs) are hollow, porous 2-4 μm microspheres derived from the cell walls of Bakers yeast. The glucan content on the surface of the particles allows for receptor mediated cell uptake by cells with β-glucan receptors, such as macrophages and dendritic cells in the immune system. GPs have been used for the delivery of macromolecules encapsulated inside the hollow GPs via layer-by-layer (LbL) synthesis. In this project, the outer surface of GPs was chemically derivatized to introduce different charged functional groups (i.e. amine, carboxylate, phosphate, and sulfate). These derivatized GPs could be potentially used for the delivery of payload drugs covalently or electrostatically bound to the GP. The modified GPs were evaluated for charged nanoparticle (i.e. aminated latex and carboxylated polystyrene nanoparticles) and soluble payload (i.e. siRNA, doxorubicin) surface binding and for efficient GP-mediated payload delivery to a model murine GP phagocytic cell line (NIH 3T3-D1).

Table of Contents

Table of Figures

Introduction

1. Glucan Particles

Glucan Particles, or GPs, are porous, hollow microspheres that are prepared from *Sacharomyces cerevisiae* (Bakers yeast). By a series of chemical extractions, the contents of the Bakers yeast cells are completely removed, leaving empty, hollow, porous microspheres (Figure 1A).

Depending on the yeast source and the chemical conditions of the extraction, GPs can be prepared with different ratios of glucan, mannan, chitosan/chitin, and lipid layer. The glucan microspheres have an average diameter of 2-4 microns and are composed of 1,3-D-Glucan and low levels of chitin (Figure 1B).

The glucan content on the surface of the particles allows receptor mediated cell uptake by cells with β-glucan receptors (dectin-1 (D1) receptor and complement receptor 3 (CR3))[i], such as macrophages and dendritic cells in the immune system. This ability to target cells in the immune system, and subsequently, cells in the blood distribution, makes the glucan particle an attractive drug delivery vehicle.

1.1 Use of Glucan Particles for Macromolecular Drug Delivery

Due to their hollow and porous nature, GPs have been used as an encapsulation device for the transport, delivery, and release of electrostatically bound particles. To deliver payload macromolecules such as DNA, siRNA, and proteins, the payload is encapsulated in the glucan particle using a layer-by-layer approach to create the polyplexes that protect the payload molecule until it is released inside the cells. Three

types of formulations as shown in Figure 2A can be prepared depending on the location of the payload molecule inside the GP encapsulated polyplex.

As a DNA delivery system, GPs meet three common needs: the particles protect DNA against nuclease degradation, deliver the DNA through the plasma membrane into the nucleus of target cells, and have minimal harmful effects. Using the GPs for DNA delivery in vitro it was possible to reduce the amount of DNA to about 10% of what is normally used with other delivery methods. Polyethylenimine (PEI) was used as the trapping polymer coats in the original studies to demonstrate the use of GP for DNA delivery. PEI allows for DNA payload protection and for endosomal release as PEI has a proton-sponge effect. The limitation in the use of PEI is related to its cytotoxicity. Currently, research is being conducted to find polymers with equal or better efficiency and reduced toxicity.[ii]

GPs with encapsulated DNA were synthesized using the LbL approach and assessed by testing the mediated delivery of the plasmid gWizGFP to NIH 3T3-D1 cells. DNA in the optimized yeast cell wall particle system efficiently transfects the 3T3-D1 cells. Greater than 50% of the cells were transfected by a 125ng DNA per $5x10^5$ cell ratio when using the encapsulated DNA. Using unencapsulated DNA/PEI nanocomplexes provides the same transfection efficiency when using a 16-fold higher concentration of plasmid DNA delivered per cell.[iii]

Preparing GPs for siRNA delivery follows a very similar approach to DNA delivery. The GP provides an encapsulation system that protects the siRNA from nuclease degradation. A co-delivery system of GP formulations with green fluorescent protein (GFP) DNA and GFP siRNA showed lower transfection efficiency than a

codelivery system using GFP DNA and scrambled siRNA in 3T3-D1 cells. The level of GFP silencing is dependent upon the siRNA concentration.[iv]

A significant advance in the use of glucan particles for siRNA delivery was the successful oral delivery of siRNA targeting map4k4 to treat inflammation in diabetic mice.[v] The first generation of particles consisted of five components: tRNA core, PEI (2 layers), Endo-Porter amphipathic peptide (EP), siRNA, and the glucan shell. These components were assembled into β-1,3-D-Glucan encapsulated siRNA particles (GeRPs) using a LbL approach. The EP is designed to be an alpha-helical, amphipathic peptide with one face being aliphatic and lipophilic and the other face being composed of basic amino acids, approximately 70% histidines. The two layers of PEI showed low toxicity, but its inclusion in the GeRPs limited the clinical applications of the particles. These original GeRPs have also been difficult to synthesis with uniformity and tend to be unstable. Newer simplified GeRPs were synthesized with only two components and without the inclusion of the PEI trapping polymer. Contrary to what was originally believed, the EP peptide is required for the silencing of targeted gene expression in macrophages. Complexes of various sizes are formed when EP binds to siRNA. These various complexes can silence gene expression in many types of cells, including macrophages and adipocytes. The gene silencing is limited to cells that have phagocytosed the GeRPs in vitro.[vi]

GPs have also been used for the encapsulation of small molecules, including Rifampicin (Rif), an antibiotic used for the treatment of tuberculosis (Tb). Rif is a neutral molecule, so it cannot be trapped inside the GP using the polyplex formation or the LbL approach. The synthetic method for encapsulating Rif inside GPs is a physical

entrapment that embeds the Rif payload in a hydrogel that partially seals the GP pores to prevent rapid drug release. The hydrogels are high-water content materials that are prepared from cross-linked, biodegradable, biocompatible, and non-toxic polymers. GP samples without a chitosan or alginate hydrogel seal release more than 90% of the encapsulated Rif within 30 minutes. GPs with the hydrogel seal showed a slower release rate, with GPs that were sealed multiple times showing the slowest rate. At pH 7, the GP-Rif formulations released up to 95% of the encapsulated Rif within 48 hours. The slow release of the drug at pH 7 is evidence that the hydrogel is not sealing 100% of the GP pores.

In addition to the use of the hollow cavity of GPs for drug encapsulation, the surface of the GP offers another option for drug binding. Chemical derivatization of the GP surface is under investigation to introduce targeting ligands to increase cell tropism of the particles, derivatization of polymers for covalent and non-covalent binding of payload drugs or nanoparticles containing a payload drug.

1.2 Surface Derivatization of GPs

Basic synthetic procedures for the surface derivatization of glucan particles, i.e. reductive amination[vii] and click chemistry[viii], allows for many different molecules and polymers to be added to the surface. These molecules can include ionic, hydrophobic, azide, or protein components, or more specifically, molecules such as biotin and cyclodextrin. Figure 2B details the basic synthesis and surface modification strategies of GPs.

The GPs can be derivatized with molecules that are used as universal surface acceptors for the attachment of ligands for specific chemical reactions. An example of

this type of derivatization is GPs derivatized with cyclodextrin, which interact with ligands bearing adamantane via a host-guest interaction. GPs derivatized with biotin can bind ligands through biotin-avidin or biotin-streptavidin interactions.[ix]

GPs that are prepared with cationic and anionic polymers on the surface of the particle can serve a multitude of purposes. These particles can bind ionic nanoparticles as well as ionic soluble payloads. The ionic soluble payloads can include drugs such as doxorubicin, a chemotherapy drug, as well as polymers such as DNA, tRNA, and siRNA. The bound payloads can be delivered by the glucan particles to cells with β-glucan receptors. The following experiments detail the synthesis and analysis of a library of cationic and anionic GPs used for electrostatic binding and delivery of ionic nanoparticles and soluble payloads to a model cell line (NIH 3T3-D1).

Materials and Methods

All materials, abbreviations, CAS numbers or Item numbers, and suppliers of products can be found in Figure 3.

1. Quality Control of Fluorescent Nanoparticles

The fluorescent polystyrene nanoparticles were used in six sizes: 20nm, 100nm, 200nm, 500nm, 1μm, and 2μm. The fluorescence excitation and emission of the fluorescent polystyrene nanoparticles was measured. Excitation was measured from 400-750nm and emission was measured from the excitation point (500nm) to 750nm. The fluorescent latex nanoparticles were used in two sizes: 100nm and 1 μm. Dilutions of the nanoparticles in saline (0.9%) were made and fluorescence measurements (excitation and emission) were made to determine the values used in future experiments using these nanoparticles. Excitation of the nanoparticles was measured from 400-750nm and emission was measured from the excitation point (500nm) to 750nm. The excitation and emission of the fluorescent polystyrene nanoparticles are detailed in Figure 4. The excitation and emission of the fluorescent latex nanoparticles are detailed in Figure 5.

2. Surface Functionalization of GPs

2.1 Synthesis of Cationic GPs

GPs (200 mg) were resuspended in 20 mL of water using a polytron homogenizer, and additional water (20 mL) was added. The particles were centrifuged at 3000 rpm for 15 minutes. The water supernatant was discarded and the particles were resuspended in water (20 mL). After resuspending, potassium periodate solution (8 mL of 1 mg/mL

solution) and additional water (12 mL) were added. The mixture was stirred in the dark at room temperature overnight. The oxidized GP sample was washed three times with water, and used immediately for reductive amination synthesis.

2.1.1 GP Surface Modification with Primary, Secondary, and Tertiary Amines (PEIs, Chitosan, & PLL)

The indicated amounts of polymer and water were added to each of the oxidized GP samples (20 mg), the particles were resuspended and mixed at room temperature overnight (Figure 6A).

After 24 hours, the samples were taken off of the rotator and allowed to rest. Sodium borohydride (1.2 g) was added to each centrifuge tube, and the tubes were allowed to sit uncapped for 24-72 hours. The PEI-GP and PLL-GP samples were washed three times with water (50 mL), while the CN-GP sample was washed three times in 0.1M acetic acid (50 mL). Tris buffer (6.5 mL of pH 7.5 solution) was added to all tubes. Water was added to total 20 mL, the particles were resuspended, and the mixture was allowed to sit for 30 minutes. The samples were again washed three times with water, resuspended in 70% ethanol, and stored overnight at -20°C for sterilization. The samples were aseptically washed three times with 0.9% saline, resuspended in 20 mL of 0.9% saline, particles were counted with a hematocytometer and the particle suspensions were diluted to a concentration of $1x10^8$ part/mL. The cationic GP suspensions were stored at -20°C.

2.1.2 Synthesis of Quaternary Amines (Quaternized Chitosan & Quaternized GP)

GPs and CN-GP were modified to introduce quaternary amines following a procedure reported for the synthesis of quaternized chitosan.[x,xi]

GP (5 mg) and CN-GP (5 mg) samples were weighed in Eppendorf tubes and resuspended in water (500 μL). Glycidyltrimethylammonium chloride (GTMAC) and water were added to each tube in the indicated amounts (Figure 6B).

The particle suspensions were incubated for 4 hours at 80°C, transferred to 15 mL centrifuge tubes with 4 mL of cold acetone, and stirred overnight at 4°C. The sample were centrifuged, washed three times with acetone, resuspended in 70% ethanol, and stored overnight at -20°C for sterilization. The sterile particles were aseptically washed three times with 0.9% saline, counted using a hematocytometer, and the particle suspensions were diluted to a concentration of $1x10^8$ part/mL. The modified GP suspensions were stored at -20°C.

2.2 Synthesis of Anionic GPs

Anionic residues cannot be directly attached to GPs or oxidized GPs. An alternative strategy was used to first derivatize the surface of GPs with amine groups and then to incorporate anionic polymers via reductive amination, EDC coupling, or photochemical crosslinking of the polymer to the amine groups of the surface. Diaminopropane (DAP) was used to generate GPs with amino groups for anionic GP synthesis. DAP-GP was synthesized by a reductive amination approach as described previously for cationic polymers (PEI-GP, CN-GP, and PLL-GP) (Section 1.1.1).

The indicated amounts of DAP and water were added, the particles were resuspended, and the mixture stirred at room temperature overnight (Figure 7A).

The mixture was taken off of the rotator and allowed to rest. Sodium borohydride (1.2 g) was added and the mixture was allowed to sit uncapped at room temperature for 24-72 hours. The samples were washed three times with water and the particles were

resuspended in Tris buffer (6.5 mL of pH 7.5 solution) and water to total 20 mL. The mixture stirred for 30 minutes, and the particles were washed an additional three times with water. The DAP-GP sample was lyophilized and stored at room temperature.

2.2.1 Synthesis of Carboxylate (Alginate-GP)

Oxidized GP was derivatized with diaminopropane (DAP), and the DAP-GP was used for EDC crosslinking of alginate to the GP surface. Alginate was dissolved in water to make a 10 mg/mL solution. The EDC and MES buffer were added to the alginate samples and stirred for 30 minutes. The indicated amount of DAP-GP was added and the samples stirred overnight at room temperature (Figure 7B).

The alginate samples were washed three times with water, the particles were resuspended in 70% ethanol, and stored overnight at -20°C for sterilization. The sterile particles were aseptically washed three times with 0.9% saline, counted with a hematocytometer, and the particle suspensions were diluted to a concentration of $1x10^8$ part/mL and particle suspensions were stored at -20°C.

2.2.2. Synthesis of Phosphate (tRNA-GP)

A solution (1 mL of 10mM) of the crosslinker sulfoSANPAH was prepared in PBS (pH 7). GP (10 mg) and DAP-GP (10 mg) were weighed in Eppendorf tubes and the indicated amount of the sulfoSANPAH solution was added to each tube (Figure 7C).

The particles were resuspended in the sulfoSANPAH solution and incubated at room temperature for 2 hours. After 2 hours, the particles were washed three times and resuspended in water (1 mL). The particles were transferred to a petri dish and tRNA (5 mL of a 1 mg/mL solution) was added and the particles were irradiated for 1 minute with a visible spectrum 350 W lamp. The samples were transferred back to 15 mL

centrifuge tubes, washed three times with water, resuspended in 70% ethanol, and stored overnight at -20°C for sterilization. The sterile particles were aseptically washed three times with sterile saline, counted using a hematocytometer, and diluted to $1x10^8$ part/mL.

2.2.3 Synthesis of Sulfate (Dextran Sulfate & Heparin)

Dextran sulfate (DS) (50 mg) and heparin (Hep) (50 mg) were resuspended in 20 mL of water and potassium periodate (12.5 mL of 1 mg/mL solution) was added. The samples were stirred overnight at room temperature in the dark. The samples were transferred to dialysis membranes (MW cutoff = 3000). The membranes were placed in separate water baths (~1 L) for 24 hours and the water was changed four times. The liquid inside the membranes was transferred to new, tared 50 mL centrifuge tubes and lyophilized. The lyophilized samples of DS and Hep were dissolved in water to create 2 mg/mL solutions. DAP-GP was dissolved in water to make a 10 mg/mL solution. The indicated amounts of DS, Hep, and DAP-GP were mixed and the samples stirred overnight at room temperature (Figure 7D).

Sodium borohydride (100 mg) was added to the DS-DAP-GP and Hep-DAP-GP samples. These samples sat uncapped for 24 hours to allow excess H_2 to escape. The samples were washed three times with water and the particles were resuspended in 70% ethanol and stored at -20°C for sterilization. The sterile samples were washed aseptically three times with 0.9% saline. The particles were counted using a hematocytometer and $1x10^8$ part/mL dilutions were made.

3. Characterization of Cationic and Anionic GPs

3.1 Ninhydrin Assay

The ninhydrin assay was used to evaluate the amount of primary and secondary amines in synthesized compounds. The ninhydrin reacts with primary and secondary amines to form Ruhemann's purple, a blue-purple colored chromophore (Figure 8). The absorbance of this ion can be measured at 570 nanometers.

A standard solution of glycine (50 mM) in glacial acetic acid was prepared. A solution of ninhydrin (2%) in DMSO was also prepared. GP samples (1-5 mg) were transferred to 1 mL centrifuge tubes. Samples were prepared from dry GPs or from suspensions in 0.9% saline. The saline suspensions were centrifuged, and the saline was removed. Water and ninhydrin were added to the tubes to a total volume of 200 μL. A calibration curve was prepared using glycine/ninhydrin solutions.

The tubes were incubated at 100°C for 10 minutes and then cooled at room temperature for 10 minutes. Ethanol (800 μL) was added to each tube and the samples were vortexed. The samples (150 μL each) were transferred to a clear-bottomed 96-well plate. Additionally, 1:5 dilutions of the samples were made in the same well plate. Absorbance of the samples was read at 570 nm with a reference wavelength of 700 nm.

3.2 Binding Assay

Fluorescent ligand binding assays were used to evaluate the binding capacity of synthesized cationic and anionic GPs. Two types of fluorescent ligand classes were evaluated for binding: (1) nanoparticles and (2) soluble polymers (i.e. tRNA, siRNA, PEI) or small drug molecules (doxorubicin).

For example, nanoparticle binding assays were used to quantify the binding capacity of synthesized cationic particles. A negative control of unmodified GP was used. Saline (0.9%), GP, and payload (nanoparticles of different diameter and different NP/GP ratios) were mixed in 1 mL centrifuge tubes and incubated in the dark for 1+ hours.

After the incubation period of 1 hour, the unbound nanoparticles were separated from the GPs containing bound nanoparticles by two methods:

(1) - Samples were centrifuged (10000 rpm for 10 minutes) and the supernatant (90 μL) was transferred to Row A of a 96 well plate, leaving the pellet in the centrifuge tube. Saline (90 μL) was added to each tube, the tubes were sonicated to resuspend particles and centrifuged. The supernatant (90 μL) was transferred to row B and 0.9% Saline (90 μL) was added. The samples were sonicated and 100 μL from each tube was transferred to Row C.

(2) - Sucrose cushion assay: To each sample was carefully added 20% sucrose (100 μL). The samples were centrifuged (3000 rpm for 10 minutes) and the supernatant (180 μL) was transferred to a 96-well plate. Saline (180 μL) was added to each tube, the samples were sonicated to resuspend particles, and centrifuged (10000 rpm for 10 minutes). The supernatant (180 μL) was transferred the well plate and 0.9% Saline (180 μL) was added to each tube. The samples were again sonicated to resuspend particles and 200 μL from each tube was transferred the well plate.

Controls totaling 100 μL were made. In well 1, 0.9% saline was added. Well 2 contained a 9:1 ratio of 0.9% Saline: 10^{10} nanoparticles, and well 3 contained a 9:1 ration

of 0.9% Saline: 10^9 nanoparticles. Finally, in well 4, a control of 9:1 0.9% Saline: 10^8 nanoparticles was made.

Fluorescent carboxylated polystyrene nanoparticles were used to evaluate binding to cationic GPs and fluorescent amine modified latex nanoparticles were used to evaluate binding to anionic GPs

3.3 Binding/Release Assay

Whereas the binding assay was used to evaluate the binding capacity of the synthesized GP compounds, the binding and release assay was used to evaluate both the binding capacity of the GP compound as well as the rate of release of the nanoparticles from GPs at different pH.

The indicated amounts of 0.9% saline, GP, and polystyrene nanoparticles were added to 1 mL centrifuge tubes and incubated for 1+ hours. After the 1+ hour incubation period, the samples were centrifuged at 10000 rpm for 3 minutes and the supernatant (90 μL) was removed and transferred to row A of a 96-well plate. The particles were resuspended in 400 μL of the indicated release assay and incubated for an additional hour. After the second incubation period, the samples were centrifuged, 100 μL was collected and transferred to row B of the well plate, leaving the pellet in the tube. The remaining 300 μL were left to incubate overnight and 100 μL samples were collected at 24 and 48 hours. The pellets were resuspended in 100 μL 0.9% saline and transferred to the well plate. The fluorescence of the supernatant and the pellets were measured from an excitation wavelength of 580 nm to an emission wavelength of 605 nm.

3.4 Zeta Potential

Zeta potential was used to estimate the charge of particles and nanoparticles. The zeta potential of NP-GP and GP samples were determined with a Malvern Zetasizer Nano-ZS (Malvern Instruments, Worcestershire, UK). Solvents and buffers were filtered through a 0.22 μm filter before sample preparation. A suspension of particles ($2x10^6$ particles/mL) was diluted in 1 mL of 20 mM Hepes buffer, vortexed and transferred to a 1 mL clear zeta potential cuvette (DTS1061, Malvern). Zeta potential was collected at 25 °C from -150 to +150 mV. The results are the average of 30 measurements collected and analyzed with the Dispersion Technology software 4.20 (Malvern) producing diagrams of zeta potential distribution versus total counts.

3.5 Flow Cytometry (FACS)

FACS measurements were obtained with a Becton Dickinson FACSCalibur instrument (BD, Franklin Lakes, NJ). Samples were prepared for FACS analysis by binding of $2x10^7$ nanoparticles to $2x10^6$ GP particles. The samples were washed from unbound nanoparticles and resuspended at $2x10^6$ GP/mL in PBS. Unmodified GPs were used as negative controls and rhodamine labeled GPs as the positive control. The particles were analyzed with an FL4 laser at 605 nm by collecting an average of 15000 measurements. Gating and analysis was performed using FlowJo 6.4.2 software.

4. Applications of Surface Derivatized GPs

4.1 Use of Cationic GPs for DNA Transfection

Cationic GPs were evaluated for efficient delivery of plasmid gWizGFP DNA into 3T3-D1 cells.

The indicated amounts of saline, GP, and gWizGFP DNA were mixed in Eppendorf tubes and incubated at room temperature in the dark for 1 hour. 10k PEI was added, while vortexing, to the indicated tubes and the samples incubated for an additional 20 minutes. The samples were washed with saline and the supernatant (90 μL) was discarded. The samples were resuspended in saline (90 μL) and DMEM (250 μL) was added. The samples were transferred to the indicated wells and the cells incubated overnight at 37˚C and 5% CO_2. After 24 hours, the media was changed and the cells incubated an additional 24 hours. The cell were fixed with 1% formalin and evaluated for frequency (% fluorescent cells) of green fluorescent protein (GFP) transfection.

4.2 Use of Anionic GPs for Doxorubicin Delivery

Doxorubicin (Dox), a cationic drug used for cancer chemotherapy, was used in binding assays and cell uptake experiments.

The indicated amounts of saline, GP, and Dox were mixed in Eppendorf tubes and incubated at room temperature in the dark for 1 hour. The samples were washed with saline and the supernatant (180 μL) was removed. The pellet was resuspended in saline (180 μL) and DMEM (250 μL) was added. The samples were transferred to the indicated wells and incubated overnight at 37˚C and 5% CO_2. The cells were fixed with 1% formalin and evaluated for evidence of GP mediated delivery of Dox.

5. Click Chemistry Derivatization of GPs

A click chemistry reaction was used to modify the surface functionality of the GPs. Before carrying out the click chemistry reaction, GPs and azido-GPs with fluorescent tRNA/PEI cores were synthesized. To make the fluorescent particles, the

indicated amount of tRNA solution was added to 1mg blanks of GP and azido-GP in microcentrifuge tubes (Figure 9).

Each tube was mixed with a heat-sealed blunt pipet tip to form a uniform wet paste. The samples were incubated for 1+ hours at 50°C. After the incubation period, the samples were lyophilized. Water (5 μL) was added and the samples were again incubated for 1+ hours at 50°C followed by lyophilization. After the second lyophilization, 0.1% PEI (5 μL) was added to the microcentrifuge tubes, a wet paste was achieved, and the samples were incubated for 10 minutes at room temperature. The indicated amount of PEI (Table 9) was added to the samples. The samples were then sonicated and incubated at room temperature for 30 minutes. After this incubation period, the samples were centrifuged, the supernatant was removed, and the particles were resuspended in 0.9% saline (1 mL). The samples were centrifuged, the saline was removed and the samples were resuspended in 70% ethanol (1 mL) and stored overnight at -20°C for sterilization. After sterilization, the samples were washed three times with sterile 0.9% saline, the particles were counted and $1x10^8$ particles/mL dilutions were prepared. The final samples were stored at -20°C.

The fluorescent tRNA core samples were used in the click chemistry synthesis. The $1x10^8$ particles/mL solutions (500 μL) were transferred to new 1 mL centrifuge tubes. The samples were centrifuged, the saline supernatant was removed, and the particles were resuspended in sterile water (500 μL). The fluorescent alkyne (500 μL) was added to each tube. Additionally, $CuSO_4$ (15 μL of 10 mg/mL solution) and sodium ascorbate (30 μL of 5 mg/mL solution) were added to each centrifuge tube. The reaction was stirred in the dark at room temperature for 3+ hours. After 3+ hours, the samples

were centrifuged, the supernatant was removed, and the samples were washed three times with water. The particles were resuspended in 0.9% saline (1 mL). Fluorescence was measured for rhodamine and GFP and the samples were analyzed under the fluorescent microscope.

Results and Discussion

1. Synthesis of Cationic and Anionic GPs

Cationic polymers such as PEI have been added to the surface of GPs, creating a payload-binding mechanism. In addition to cationic polymers, anionic polymers can also be added to the surface of GPs. In order to attach the components of nanoparticles to the outside of the glucan particles, the GP must first be oxidized to activate the carbohydrate surface. After the oxidation, cationic groups can be covalently grafted to the surface, while the addition of most anionic groups need an additional linker such as diaminopropane, DAP, in order to be attached to the surface of the GP.

Once functional groups have been added to the surface of the GP, the particles can be further modified to better serve the binding needs. For example, chitosan attached to the surface of GP can be modified in order to produce quaternary amines.

The success of the synthesis of the cationic and anionic GPs was characterized using the ninhydrin assay and zeta potential measurements.

1.1 Ninhydrin Assay Results

To determine the amount of primary and secondary amines in synthesized GPs, the ninhydrin assay was used. The ninhydrin reacts with primary and secondary amines, creating the chromophore Ruhemann's purple. This chromophore can be measured using absorbance. The results of the ninhydrin assay, including unmodified GP and synthesized GP compounds, are summarized in Figure 10.

The ninhydrin assay results show that most GPs modified by reductive amination have a higher molar content of amines as compared to the unmodified GP control. An

unmodified GP is composed of 1-2% chitosan, the amines of the chitosan account for the low levels of NH_2 measured in the GP control. A slight increase in the NH_2 content for the PEIs, CN, and PLL modified particles confirms surface modification. A limitation of the ninhydrin assay is that it does not react with tertiary or quaternary amines. Overall, the measurements of μmol NH_2 represent the modified particles, with the exception of DAP-GP. DAP-GP should have a relative high level of NH_2, but measurements show that the concentration of amines is very low. The size of the DAP molecule may be contributing to this measurement, as the DAP may be embedded in the GP matrix, where steric hindrance limits reaction with ninhydrin.

1.2 Zeta Potential Results

To determine an estimate of the charge of the glucan particles, zeta potential measurements were used. The particles were suspended in filtered Hepes buffer and measured using a Zetasizer at 25 °C from -150 to +150 mV. The zeta potential measurements of unmodified GP and synthesized cationic and anionic GP compounds are summarized in Figures 11A and 12A. All values are +/- 5mV.

The unmodified GP control has a neutral zeta potential, and shifts of more than 10mV to positive zeta potential confirms the synthesis of cationic GPs (Figure 11A). An example of cationic surface modification confirmed by zeta potential is shown in Figure 11B. The zeta potential measurements are an estimate of the charge of the particle. An ideal particle will not aggregate unless centrifuged. GPs, however, aggregate over time. The particle aggregation inside the zeta potential cell can have a negative effect on measuring the true potential of the particle. Aggregation of modified GPs masks some of the surface charge of the particles, resulting in a smaller shift of zeta potential.

Anionic polymers cannot be immediately added to the surface of GPs or oxidized GPs. The strategy used to create modified anionic GPs was to derivatize the surface with amine groups so the anionic polymers could be incorporate using reductive amination, EDC coupling, or photochemical crosslinking. DAP-GP was successfully prepared as confirmed by its cationic (19.6 mV) zeta potential. For some particles the shift in zeta potential to anionic value was minimal indicating low yield of polymer grafting to the DAP-GP. The reductive amination was used to synthesize the DS-DAP-GP (12.1 mV) and Hep-DAP-GP (10.0 mV) particles. The reductive amination gives lower yields and is not very efficient compared to the other strategies.

The successful derivatization of particles with the alginate polymer did depend on using DAP; the reaction was more efficient than DS-DAP-GP (12.1 mV) and Hep-DAP-GP (10.0 mV) due to the EDC crosslinking. Crosslinking by EDC will not take place unless amine groups are on the surface of the GP. Thus, the Alg-DAP-GP (-21.1 mV) and AlgL-DAP-GP (-18.2 mV) successfully bind nanoparticles and soluble polymers, while the Alg-GP (-0.71 mV) and AlgL-GP (-6.54 mV) do not. The sequential modification of GP to produce DAP-GP and finally Alg-DAP-GP was confirmed by zeta potential (Figure 12B).

The successful synthesis of the tRNA derivatized particles did not depend on DAP. The crosslinker, sulfoSANPAH, is a photo-crosslinker, which reacts with amine groups such as DAP, but also with hydroxyl groups that can be found of the surface of the unmodified GP. This is shown by the zeta potential shifts of tRNA-GP (-15.9 mV) and tRNA-DAP-GP (-16.8 mV).

2. Characterization of Cationic and Anionic GPs

Using the ninhydrin assay and zeta potential measurements, the synthesis of cationic and anionic particles was considered a success. The binding capacity of the ionic GPs was tested using binding experiments with nanoparticles.

2.1 Nanoparticles

In binding experiments with synthesized GPs, two types of nanoparticles (NPs) were used. When testing cationic GPs, anionic (carboxylated) fluorescent polystyrene nanoparticles were used. Fluorescent cationic (amine) latex nanoparticles were used when testing the binding capacity of anionic GPs.

2.2 Nanoparticle Binding to GPs

2.2.1 Polystyrene Nanoparticles

To determine the binding capacity of the cationic GPs, all sizes (0.02, 0.1, 0.2, 0.5 1, and 2 μm) of polystyrene nanoparticles were bound to the synthesized GPs. The nanoparticles were incubated with the GPs for one hour, and the fluorescence of the supernatant, wash, and pellet were measured from 580-605 nm. Figures 13A, 14A, and 15A detail the measured binding capacity of the three smallest sizes of fluorescent nanoparticles.

The binding capacity is defined as the ratio of nanoparticle concentration determined from fluorescence emission measurements divided by the target input of nanoparticle concentration.

$$\frac{\text{measured NP concentration in pellet}}{\text{input NP concentration}} = \text{Binding Capacity}$$

Accurate measures of binding capacity for the larger nanoparticle sizes (0.5, 1, and 2 μm) were not quantified due to the aggregation and co-precipitation of free nanoparticles.

Particles that showed clear evidence of polystyrene nanoparticle binding were transferred to slides and examined under a fluorescence microscope at 100x. Figures 13B, 14B, and 15B show evidence of selective binding of 20nm, 100nm, and 200nm polystyrene nanoparticles to cationic GPs, but not the unmodified GP control.

Additionally, to determine the binding capacity of fluorescent particles to unmodified GP and synthesized cationic GPs, flow cytometry was used. The nanoparticles were incubated with the GPs for one hour, the pellet was resuspended in PBS, and the FACS measurements were made with a Becton Dickinson FACSCalibur instrument. The results show that unmodified GPs do not bind the fluorescent polystyrene and the modified GPs do bind the nanoparticles (Figure 16).

Finally, to determine an estimate of the shift in surface charge of the cationic GPs bound to fluorescent (anionic) polystyrene nanoparticles, zeta potential was used. The nanoparticles were incubated with the GPs for one hour, the pellet was resuspended in filtered Hepes buffer and measured using a Zetasizer at 25 °C from -150 to +150 mV. The results are detailed in Figure 17A.

The binding assay and microscopy results regarding neutral, unmodified GP were confirmed by zeta potential measurements. The zeta potential of the neutral GPs did not shift in the sample containing GPs and 200nm r-PS nanoparticles. In addition, the peak of the free NPs was measured in this sample at ~ -60 mV. For Cationic GPs, zeta potential confirms (1) binding of the anionic nanoparticles as the zeta potential of the

cationic GP shifts to an anionic value, and (2) the successful separation of unbound NPs from the NP-GP sample as there is only one peak (NP-GP) and no evidence of free polystyrene nanoparticles at ~ -60 mV. As a specific example, the zeta potential of CN-GP before and after binding to polystyrene nanoparticles is illustrated in Figure 17B.

The cationic GPs were also bound to the larger polystyrene nanoparticles: 500nm, 1μm, and 2μm. However, unbound nanoparticles aggregated with the GPs in the pellet, so accurate fluorescence measurements for binding capacity could not be collected. The samples were examined at 100x using a fluorescence microscope for evidence of nanoparticle binding. Figure 18 details cationic GPs binding the larger nanoparticles.

2.2.2 Latex Nanoparticles

To determine the binding capacity of the anionic GPs, one size of latex nanoparticles (100nm) was bound to the synthesized anionic GPs. The nanoparticles were incubated with the GPs for one hour, and the fluorescence of the supernatant, wash, and pellet were measured from 520-540 nm. The latex nanoparticles easily aggregated, resulting in an inability to accurately measure fluorescence, binding capacity, and zeta potential. The collected results, including the quality control experiments of the free particles, did not give expected results. The zeta potential of the nanoparticles bound to GPs (Figure 19C) confirms the particle aggregation, as the measurement shows data representative of the buffer control.

Due to the aggregation of the latex nanoparticles, quantitative data for the binding capacity of the anionic GPs was not easily collected (Figure 19A). Latex binding to anionic GPs was confirmed only by qualitative microscopy evaluation of the anionic GP samples and the unmodified GP control.

The aggregation of both bound and unbound latex nanoparticles in the pellet did not allow for accurate fluorescence readings. Samples were transferred to slides and examined under a fluorescence microscope at 100x. Figure 19B shows evidence of binding of 100nm latex nanoparticles to Alg-DAP-GP, but not the GP control.

2.3 Polymer Binding to GPs

When binding experiments using nanoparticles proved to be successful, the particles were used in binding experiments using fluorescent polymers or soluble payloads, including nucleic acids.

2.3.1 Nucleic Acids binding to cationic GPs

To determine the binding capacity of the cationic GPs, three different anionic polymers were used, Cy3-sirRNA, r-DNA, and r-tRNA. The polymers were incubated with the GPs for one hour, and the fluorescence of the supernatant, wash, and pellet were measured from 540-573 nm. The binding capacity results in Figure 20A proved selective binding of anionic siRNA to cationic GPs.

The binding capacity is larger for the quaternary GP which correlates with the expected result that a particle modified with quaternary amines has higher binding affinity than particles modified with primary or secondary amines. The GP control did not bind a significant amount of siRNA.

Particles that showed clear evidence of Cy3-siRNA binding were transferred to slides and examined under a fluorescence microscope at 100x. Figure 20B shows evidence of binding of Cy3-siRNA polymer.

Finally, to determine an estimate of the shift in surface charge of the cationic GPs bound to fluorescent (anionic) Cy3-siRNA, zeta potential was used. The polymer was

incubated with the GPs for one hour, the pellet was resuspended in filtered Hepes buffer and measured using a Zetasizer at 25 °C from -150 to +150 mV. The zeta potential results for GPs +/- Cy3-siRNA are detailed in Figure 20C.

The second polymer, fluorescently labeled DNA (r-DNA) was also bound to cationic GPs at a ratio of 1 μg/1x10^6 GP. The binding results in Figure 21A do not clearly confirm selective binding of r-DNA compared to the neutral GP control. A high concentration of r-DNA was necessary to obtain a strong fluorescent signal, and it is likely some of the r-DNA precipitated during the binding assay. Additional work is required to confirm binding of r-DNA to cationic GPs by using a more fluorescent sample so that the experiment can be done at similar concentrations used for siRNA.

Only the 25k PEI-GP particles show evidence of binding of r-DNA higher than that of the unmodified GP. These particles were transferred to slides and examined under a fluorescence microscope at 100x. Figure 21B shows evidence of binding of the r-DNA polymer to both cationic GP and the neutral GP control.

The r-DNA was most likely absorbed into the center of some GPs, resulting in the binding capacity of unmodified GP being higher than some of the synthesized cationic glucan particles.

The third polymer, fluorescently labeled tRNA (r-tRNA) was also bound to cationic GPs at a ration of 1 μg r-tRNA/1x10^6 GPs. Similarly to DNA, the results in Figure 22A do not show an improvement in binding capacity of tRNA to cationic GPs compared to the neutral GP control. Again, the high concentration and quality of the polymer affected the efficiency of binding.

Particles that showed clear evidence of r-tRNA binding were transferred to slides and examined under a fluorescence microscope at 100x. Figure 22B shows evidence of binding of r-tRNA.

The r-tRNA was also most likely absorbed into the center of some GPs, resulting in the binding capacity of unmodified GP being higher than some of the synthesized cationic glucan particles. Additionally, the tRNA and DNA could be precipitating and randomly binding to the unmodified GP surface or forming aggregates in the pellet. The age of the nucleic acid samples could also be a factor as the older samples are less stable.

2.3.2 10k Polyethyleneimine binding to anionic GPs

To determine the binding capacity of the anionic GPs, one cationic polymer was used, r-10k PEI. The polymers was incubated with the GPs for one hour, and the fluorescence of the supernatant, wash, and pellet were measured from 540-573 nm. Anionic GP binding assays used GPs in the amount of $1x10^8$ part/mL and r-10k PEI in a concentration of 0.1 mg/mL (1 μg PEI/$1x10^6$ GPs). The results shown in Figure 23A confirm selective binding to anionic GPs.

The expected results, based on surface charge, for binding capacity of anionic GPs predict that the heparin and dextran sulfate GPs will have the highest binding capacity, followed by the tRNA GPs, and the alginate GPs were expected to have the lowest binding capacity. However, of the anionic GPs, the alginate-GPs showed the highest binding capacity. The efficient synthesis of the Alg-DAP-GP and AlgL-DAP-GP particles using EDC crosslinking provides a high yield of particles with alginate covering the surface. The photo-crosslinking of the tRNA-GP and tRNA-DAP-GP particles using sulfoSANPAH was also an efficient synthesis, and the tRNA particles also bound

cationic polymers well. The reductive amination synthesis used to prepare the DS and Hep GPs was not nearly as efficient as the crosslinking reactions, making the binding capacity of the DS-DAP-GP and Hep-DAP-GP lower than the rest of the anionic particles.

Particles that showed clear evidence of r-10k PEI binding were transferred to slides and examined under a fluorescence microscope at 100x. Figure 23B shows evidence of binding of r-10k PEI polymer.

3. Applications of Cationic and Anionic GPs

After successful binding experiments with the polymers and soluble payloads, the cationic GPs were used in DNA transfections and the anionic GPs were used in uptake experiments using a cationic cancer drug.

3.1 DNA Transfection with Cationic GPs

To determine the transfection efficiency of cationic GPs, the particles were bound to gWizGFP DNA and delivered to 3T3-D1 cells. The cells incubated with the DNA for 48 hours and were evaluated for frequency (% fluorescent cells) of green fluorescent protein (GFP) transfection. Transfection efficiency was calculated as the percentage of fluorescent cells (cells expressing GFP) in a field containing approximately 200 cells. Figure 24A details transfection efficiency of cationic GPs with a DNA concentration of $0.5\mu g/1x10^6$ particles.

To determine the concentration of DNA that will provide the best transfection efficiency, the concentration of DNA was varied in transfection experiments. Figure 24B details the transfection efficiency of CN-GP with varying concentrations of DNA.

The CN-GP samples from the DNA transfections were examined on a fluorescence microscope for evidence of GFP DNA transfection. The CN-GP gave the best transfection results of all synthesized cationic GPs. The chitosan on the surface of the GP binds the plasmid DNA used for transfection, but it binds much less tightly than other cationic GPs, such as 10k PEI-GP, 25k PEI-GP, and Q-GP. The CN-GP will release the plasmid DNA more quickly than the other cationic GPs because the DNA is less tightly bound to the chitosan. Figure 24C shows the difference in DNA transfection efficiency with unmodified GP and CN-GP.

3.2 Doxorubicin (Dox) Delivery with Anionic GPs

To determine the binding capacity of the anionic GPs, one drug was used, doxorubicin (Dox). The Dox was incubated with the GPs for one hour, and the fluorescence of the supernatant, wash, and pellet were measured from 480-550 nm. Figure 25A shows a significantly low binding capacity (less than 20% of Dox input was bound to all particles). Dox binding to the anionic GPs was confirmed by qualitative fluorescent microscopy evaluation of all samples (Figure 25B).

To deliver the Dox to cells, the GP pellets bound to Dox were resuspended in DMEM and added to the 3T3-D1 cells. To determine the GP mediated uptake of Dox by 3T3-D1 cells, the cells were evaluated by fluorescent microscopy. Figure 25C shows the difference in fluorescence based on uptake of unmodified GP and tRNA-DAP-GP.

The anionic GPs were able to bind Dox in a moderate amount. Additionally, the anionic GPs were able to successfully deliver Dox to cells; however, the amount of Dox delivered to the NIH 3T3-D1 cells is limited by the binding capacity of the GPs. Without

more than moderate binding of Dox by anionic GPs, the expected results of the slowing of cell growth and eventual cell death will not be attained.

4. Click Chemistry Modifications of GPs

To determine the success of the click chemistry reaction, the particles were evaluate using fluorescent microscopy. The click chemistry reaction was used to modify the surface functionality of the GPs. The GPs synthesized using the click chemistry method included a positive control of GP and a negative control of azido-GP. Both particles were able to absorb the r-tRNA/PEI core and show red fluorescence inside the particles. However, only the surface of the GP was able to react with the f-alkyne to show green fluorescence of the surface of the particle (Figure 26).

The click chemistry reaction is a very selective reaction. In the past, the reaction to attach polymers and hydrocarbons to the surface would destroy the polymers encapsulated inside the particles. If the surface was derivatized first, the loading of the inside of the GP was restricted. This reaction has successfully loaded a rhodamine tRNA/PEI core inside the GP and attached a GFP alkyne to the surface of the particle.

Conclusions

The synthesized library of cationic-GPs bound fluorescent anionic polystyrene nanoparticles and nucleic acids (siRNA, DNA, tRNA). The PEI-GPs (10k and 25k) as well as the Q-GP tended to have the highest binding capacity for both the nanoparticles and the nucleic acids. The PLL-GP exhibited very low levels of binding, nearly synonymous with the unmodified GP. The cationic GPs also functionally delivered GFP expressing plasmid DNA into GP-phagocytic cells leading to efficient transfection. The CN-GP provided the best transfection efficiency due to its moderately tight binding of the plasmid DNA.

The library of anionic-GPs bound fluorescent cationic latex nanoparticles. The nanoparticle aggregation did not allow for accurate fluorescence readings or binding capacity measurements; the confirmation of the binding data was accomplished by qualitative microscopy. Additionally, the anionic GPs bound the soluble polymer rhodamine-10k PEI and the cancer chemotherapeutic drug doxorubicin. Binding of Dox provided targeted drug delivery into GP-phagocytic cells. The anionic alginate (Alg-DAP-GP and AlgL-DAP-GP) tended to show the highest binding capacity for the nanoparticles, polymers, and the drug. The anionic GPs with tRNA on the surface (tRNA-GP and tRNA-DAP-GP) showed a moderate binding capacity for all payloads. Of the anionic GPs synthesized with DAP, the dextran sulfate and heparin GPs (DS-DAP-GP and Hep-DAP-GP) showed the lowest binding capacity for all payloads. The alginate and tRNA coupling reactions to DAP-GP using the EDC and sulfoSANPAH crosslinkers, respectively, are more efficient than reductive amination of Hep and DS.

Particles showing little to no binding capacity included the alginate, dextran sulfate, and heparin particles synthesized without DAP (Alg-GP, AlgL-GP, DS-GP, and Hep-GP).

In conclusion, moderate success was achieved in the synthesis of a working library of cationic and anionic glucan particles. The particles were able to bind ionic nanoparticles, polymers, and drugs for delivery to cells. The binding capacity of few particles (25k PEI-GP, Q-GP, Alg-DAP-GP) was exceptional. Most particles showed moderate binding, and few showed little to no binding (PLL-GP, DS-GP, Hep-GP). Also, the modified glucan particles tended to bind payloads well, but the release of the payloads was sporadic and unable to be quantified. The particles with high binding capacities were successful in delivery of payloads to cells. However, the amount of payload, specifically Dox, bound to the particles was not enough to cause the expected slow of cell growth and eventual cell death. Improvements in these particles (Future Work) will take steps toward creating an ideal particle that can successfully and efficiently deliver ionic drug products and plasmid DNA to cells.

Future Work

Future work regarding the synthesis and analysis of surface derivatized glucan particles will include synthesizing surface derivatized GPs with pH sensitive, glutathione, or redox sensitive groups to control nanoparticle and drug release.

Additionally, work will be done to address problems such as the synthesis and analysis of the DAP-GP particle. DAP-GP should exhibit a higher amine content in a test such as the ninhydrin assay. However, tests have show that the amine content found in DAP-GP is similar to and occasionally lower than the unmodified GP. It is speculated that the size of DAP forces it to be embedded in the GP matrix. If embedded in the matrix, the ninhydrin cannot reach it, the reaction does not occur, and a low amine content level is observed. Extending the hydrocarbon chain on the surface of the particle using a compound like polyethylene glycol (PEG) will make the amine group of DAP more visible and more likely to react with ninhydrin.

Additional work is required to optimize use of cationic GPs for DNA transfection and siRNA delivery. Future work with anionic GPs will also be carried out to optimize Dox binding and delivery to macrophage cells.

Future improvements of the surface modification of cationic and anionic glucan particles will strive to create the ideal particle, which will not aggregate, can bind payload successfully in a significant amount, release the payload inside of cells with β-glucan receptors, and be easily degraded by the human body. Because the surface of the particles is cationic or anionic, a wide range of payloads or drugs can be electrostatically bound to the surface of the particles. The applications of these particles are not limited to cancer or chemotherapy drugs. The ideal glucan particle, because it is derived from

Bakers yeast, can provide a lower-cost, non-toxic drug delivery system for many types of drugs, possibly making the medical treatment for many diseases and conditions more affordable for people around the world.

Figures

A

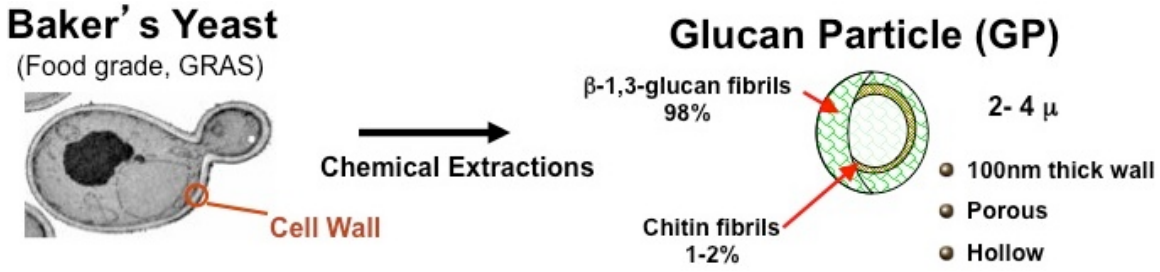

B

Composition	Particle Type		
	Glucan Particle (GP)	*Glucan Mannan Particle (GMP)*	*Yeast Chitin Particle (YCP)*
Glucan	80%	40%	40-50%
Mannan	<1%	40%	0%
Chitin	2-4%	2-4%	40-50%

Figure 1 - Glucan Particle Basics: *A*, Schematic representation of Glucan Particle (GP) synthesis. *B,* Types and Compositions of GPs.[xii] For this project, only the GP was used.

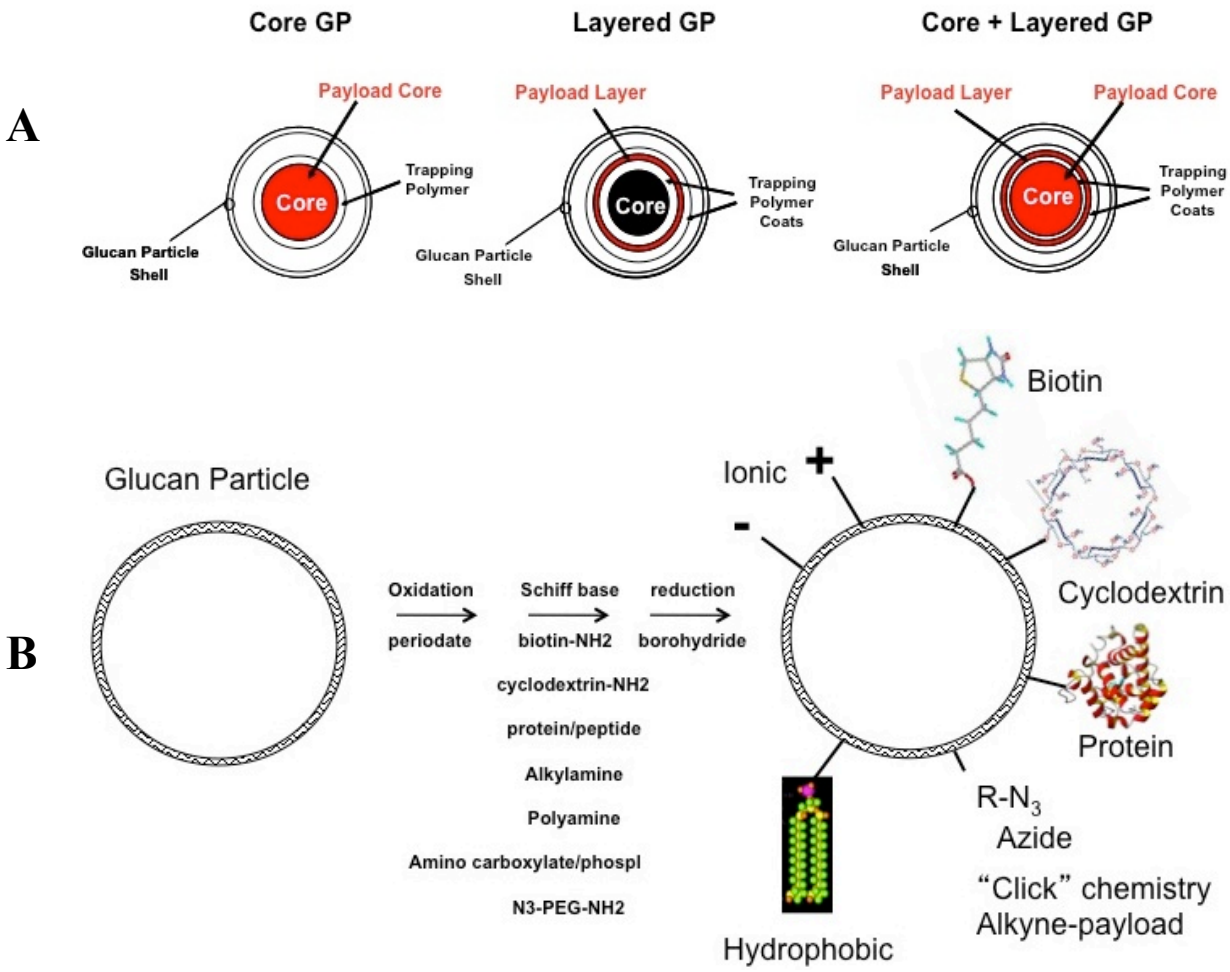

Figure 2 - GP Drug Delivery Methods: *A,* Layer-by-layer (LbL) approach for drug encapsulation inside the hollow chamber of the glucan particle. *B,* Possible surface derivatization ideas for electrostatic binding of drug particles. This project deals with creating ionic GP surfaces.

Chemical	Abbreviation	CAS No. (Product #)	Supplier
Potassium Periodate	KIO_4	7790-21-8	Sigma Aldrich
Polyethyleneimine (10k)	10k PEI	9002-98-6	Sigma Aldrich
Polyethyleneimine (25k)	25k PEI	9002-98-6	Sigma Aldrich
Chitosan from crab shells, minimum 85% deacetylated	CN	9012-76-4	Sigma Aldrich
Poly-L-lysine Hydrobromide	PLL	25988-63-0	Sigma Aldrich
Sodium Borohydride	$NaBH_4$	16940-66-2	EMD
Glycidyltrimethylammonium Chloride	GTMAC	3033-77-0	Sigma Aldrich
1,3-diaminopropane	DAP	109-76-2	Sigma Aldrich
Sodium Alginate F200	Alg	95328-14-6	Multi-Kem Corp. (Ridgefield, NJ)
Sodium Alginate F200L	AlgL		Multi-Kem Corp. (Ridgefield, NJ)
1-ethyl-3-(3-dimethylaminopropyl) carbodiimide	EDC	1892-57-5	Sigma Aldrich
Sulfosuccinimidyl 6-((4-azido-2-nitrophenyl) amino)hexanoate	sulfoSANPAH	102568-43-4	Pierce Chemicals (Rockford, IL)
Dextran Sulfate sodium salt	DS	9063-02-9	Amersham Pharmacia (Piscataway, NJ)
Heparin sodium salt from porcine intestinal mucosa	Hep	9041-08-1	Sigma Aldrich
Ninhydrin		485-47-2	Sigma Aldrich
Glycine		56-40-6	Sigma Aldrich
FluoSpheres® Size Kit #1, Carboxylate modified microspheres, red fluorescent (0.02, 0.1, 0.2, 0.5, 1, and 2 μm in diameter)	r-PS	(F8887)	Invitrogen
Latex Beads, amine modified polystyrene, fluorescent orange (0.1 and 1 μm in diameter)	Latex	(L9904)	Sigma Aldrich
Hepes, Free Acid	Hepes	7365-45-9	EMD
(8*S*,10*S*)-10-(4-amino-5-hydroxy-6-methyl-tetrahydro-2H-pyran-2-yloxy)-6,8,11-trihydroxy-8-(2-hydroxyacetyl)-1-methoxy-7,8,9,10-tetrahydrotetracen-5,12-dione (Doxorubicin)	Dox	29042-30-6	Sigma Aldrich
Copper (II) Sulfate	$CuSO_4$	7758-98-7	Sigma Aldrich
(+) sodium-L-ascorbate		134-03-2	Sigma Aldrich
Oregon Green 488 alkyne 6-isomer	f-alkyne	(O10181)	Invitrogen

Figure 3 - Materials: All materials used in the project. Also included are abbreviations, CAS or Item numbers, and suppliers.

A

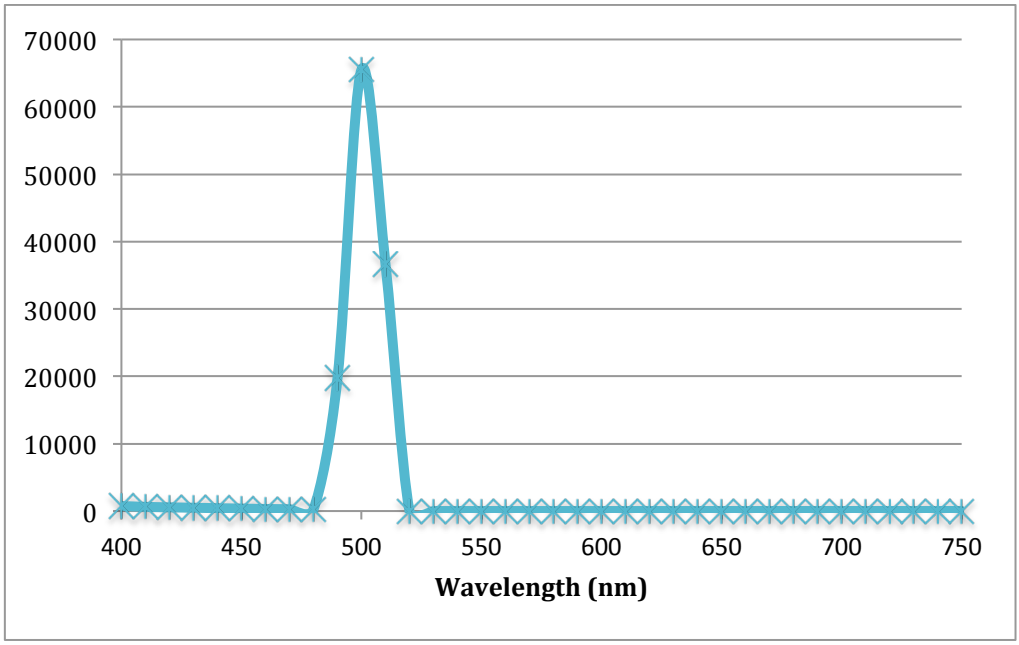

B

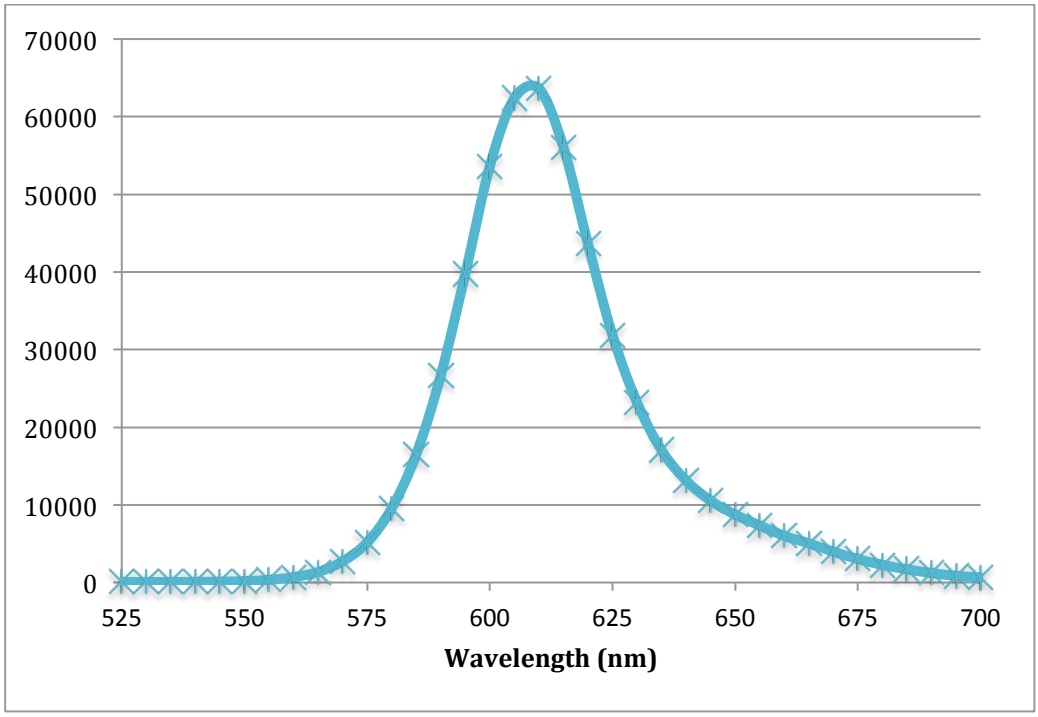

Figure 5 - Fluorescence of Polystyrene Nanoparticles: *A,* Excitation of fluorescent polystyrene nanoparticles. *B,* Emission of fluorescent polystyrene nanoparticles.

A

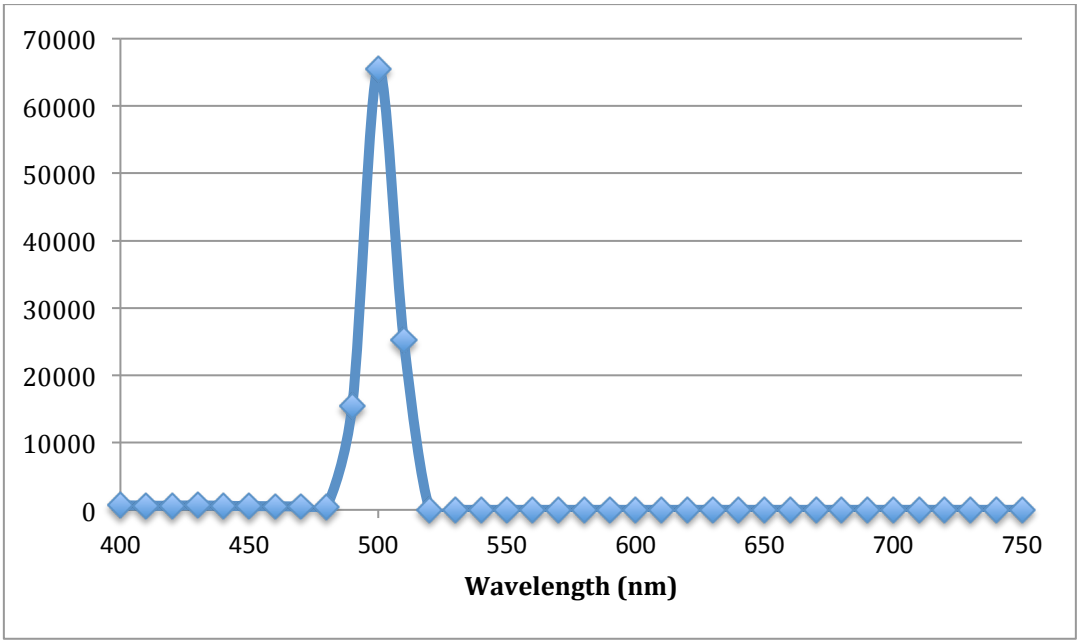

B

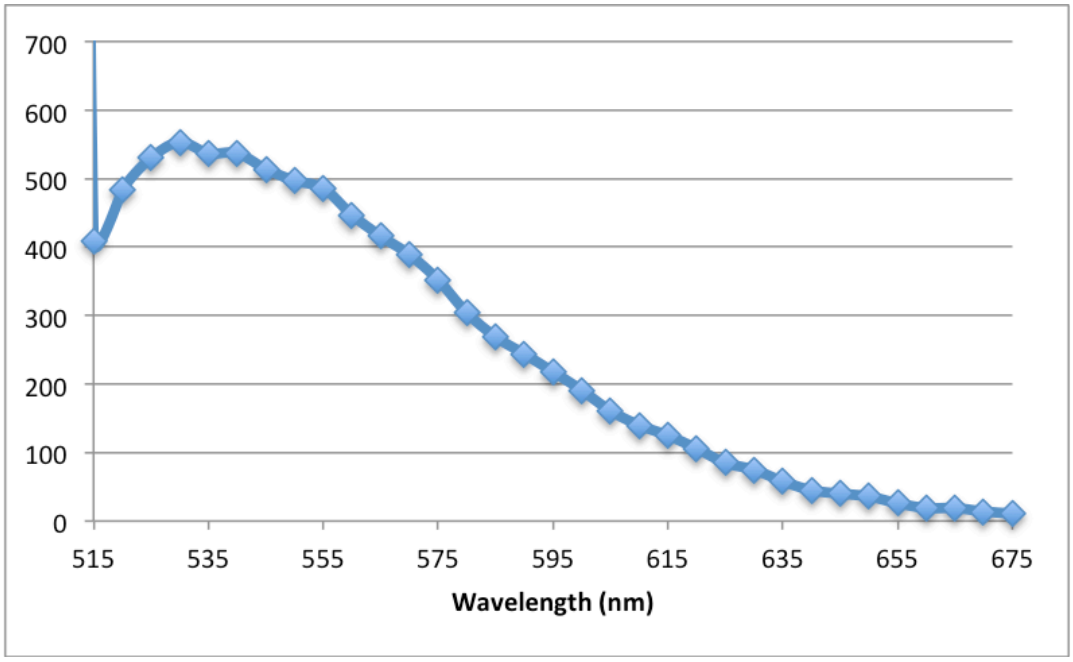

Figure 5 - Fluorescence of Latex Nanoparticles: *A,* Excitation of fluorescent latex nanoparticles. *B,* Emission of fluorescent latex nanoparticles.

A

Polymer	Abbreviation	% w/v TP	mL TP	mmol polymer	mL Water
10k PEI	10kPEI-GP	1	42.4	0.0424	2.6
25k PEI	25kPEI-GP	5	22.4	0.0448	22.6
Sigma Chitosan	CN-GP	1	42.1	0.0042	2.9
PLL	PLL-GP	1	10.0	0.0213	4.0

B

GP Sample	GTMAC/GP ratio (µL/mg GP)	mg GP	µL GTMAC	$\frac{\text{mmol GTMAC}}{\text{mg GP}}$	µL Water
GP	2	5	10	0.0149	490
GP	20	5	100	0.1490	400
GP	50	5	250	0.3726	250
GP	100	5	500	0.7452	0
CN-GP	20	5	100	0.1490	400

Figure 6 - Synthesis of Cationic GPs: *A,* Synthesis of non-quaternary cationic GPs. *B,* Synthesis of quaternary cationic GPs.

A

Polymer	% TP	mL TP	mmol DAP	mL Water
DAP	0.1	3.1	0.0418	41.9

B

Polymer	mL Alg	mL EDC (10 mg/mL)	mL MES Buffer	mL DAP-GP
Alg F-200	8	8.4	11.6	20
Alg F-200L	8	8.4	11.6	20

C

Sample	mg Sample	µL sulfoSANPAH	mL tRNA
tRNA-GP	10	500	5
tRNA-DAP-GP	10	500	5

D

Polymer	mL Polymer	mL DAP-GP
DS	20	20
Hep	10	20

Figure 7 – Synthesis of Anionic GPs: *A,* Synthesis of Diaminopropane-GP. *B,* Synthesis of Alginate (Carboxyl) GPs. *C,* Synthesis of tRNA (Phosphate) GPs. *D,* Synthesis of Dextran Sulfate and Heparin (Sulfate) GPs.

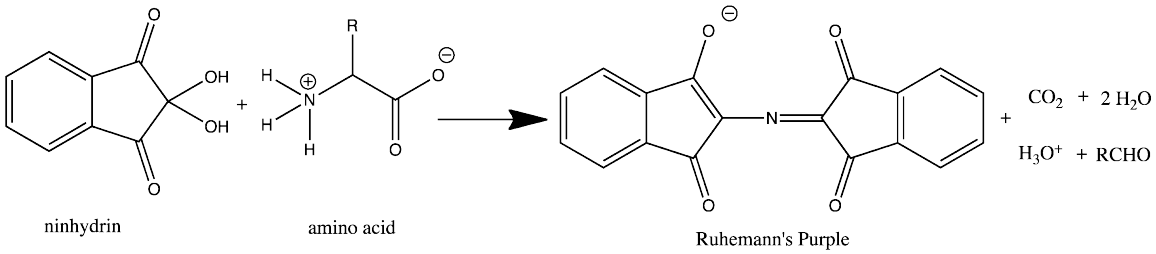

Figure 8 - Ninhydrin Reaction Scheme: The reaction of ninhydrin with an amino acid to form Ruhemann's Purple, a blue-purple colored chromophore.[xiii]

Core	µL tRNA	µL 0.1% PEI
GP-(R)tRNA/P	5 of 10 mg/mL	30
N_3-GP-(R)tRNA/P	5 of 10 mg/mL	30

Figure 9 – Click Chemistry Derivatizations of GPs: Synthesis of Click Chemistry Particles

GP Sample	$\frac{\mu mol\ NH_2}{mg\ Cationic\ GP}$
GP	0.0456 ± 0.010
10k PEI-GP	0.0820 ± 0.004
25k PEI-GP	0.0865 ± 0.006
CN-GP	0.0728 ± 0.006
DAP-GP	0.0278 ± 0.015
PLL-GP	0.1185 ± 0.011
Q-GP	0.0683 ± 0.021

Figure 10 - Ninhydrin Assay Results: Results of the Ninhydrin Assay, listed in micromoles of amine per milligram of cationic GP tested.

A

GP Sample	Zeta Potential Maximum
GP	-2.09
10k PEI-GP	17.6
25k PEI-GP	19.2
CN-GP	21.0
DAP-GP	19.6
PLL-GP	9.01
Q-GP	19.6

B

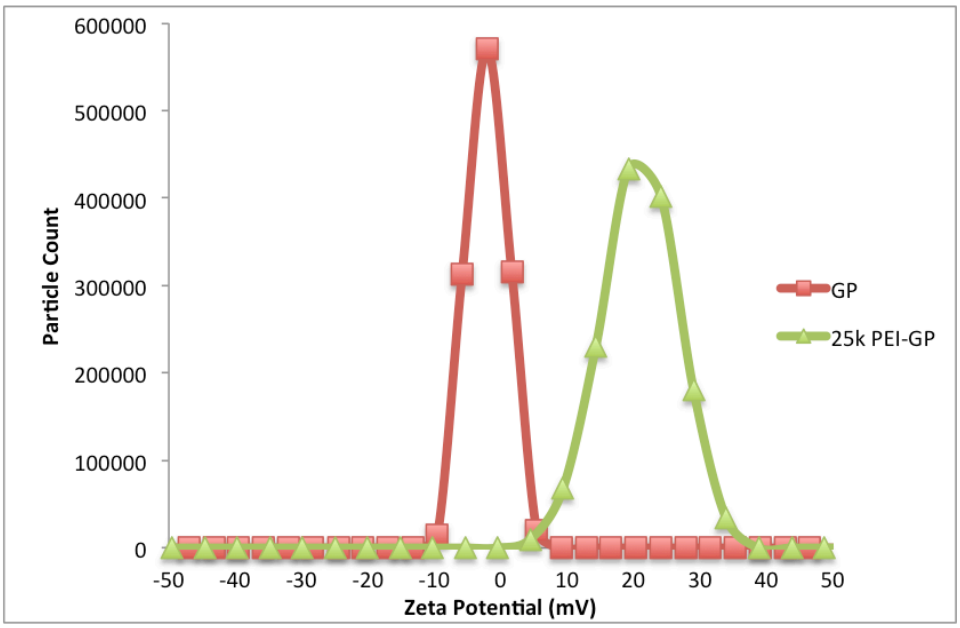

Figure 11 - Zeta Potential Results for Cationic GPs: *A,* Zeta potentials for all synthesized cationic GPs. *B,* A sample plot of the zeta potential shift of cationic GPs.

A

GP Sample	Zeta Potential Maximum
GP	-2.09
DAP-GP	19.6
DS-DAP-GP	12.1
DS-GP	-3.30
Hep-DAP-GP	10.0
Hep-GP	-2.43
Alg-DAP-GP	-21.1
Alg-GP	-0.71
AlgL-DAP-GP	-18.2
AlgL-GP	-6.54
tRNA-DAP-GP	-16.8
tRNA-GP	-15.9

B

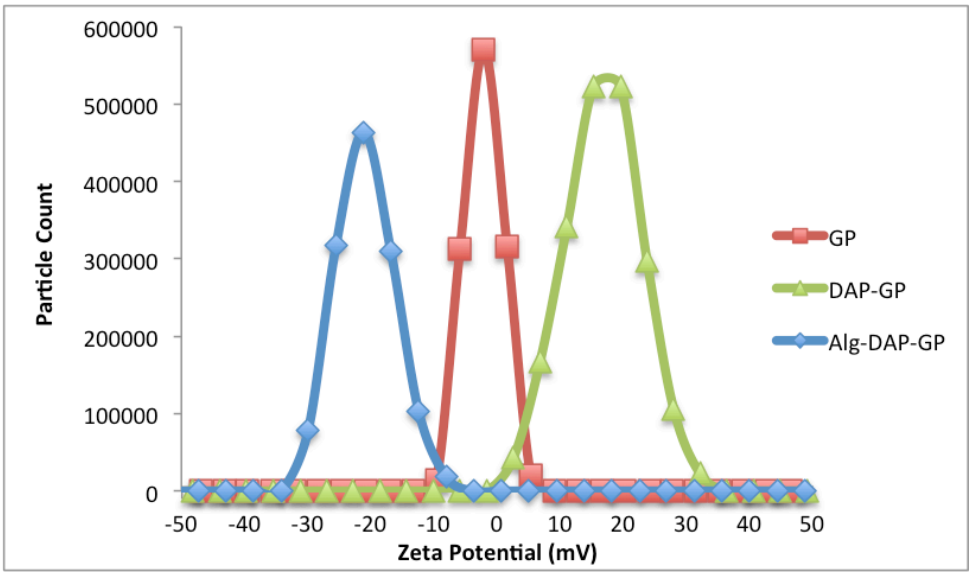

Figure 12 - Zeta Potential Results for Anionic GPs: *A,* Zeta potentials for all synthesized anionic GPs. *B,* A sample plot of the zeta potential shift of anionic GPs

A

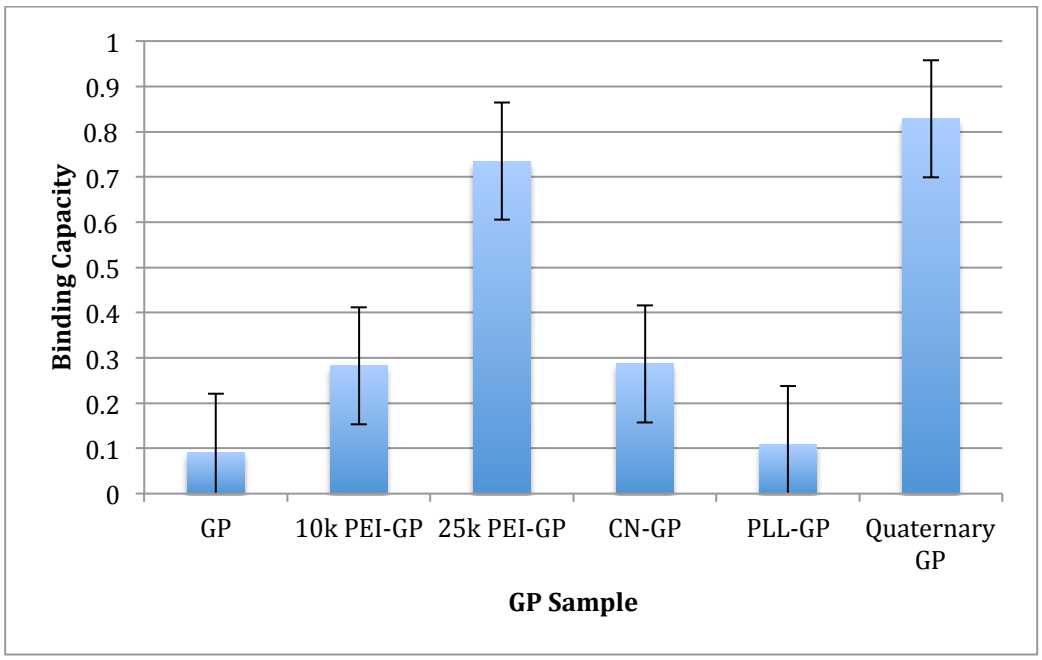

B

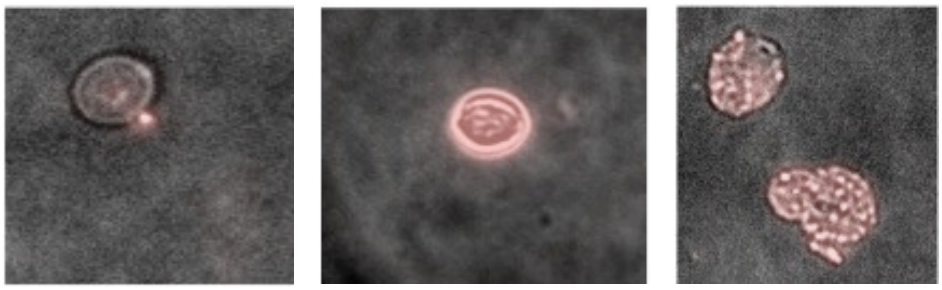

Figure 13 - Cationic GPs Binding Results with 20nm r-PS: *A,* Binding Capacity Graph showing the calculated binding capacity for cationic GPs bound to fluorescent 20nm polystyrene nanoparticles at a ratio of 100 NP/GP. *B,* Fluorescent microscopy images for 20nm r-PS bound to GP, 25k PEI-GP, and Q-GP.

A

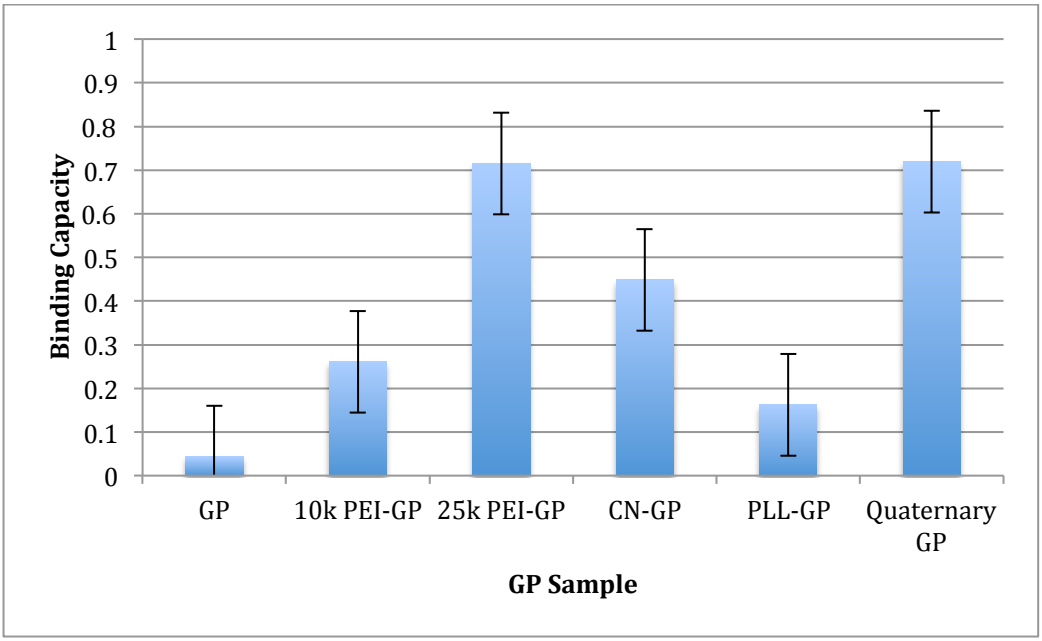

B

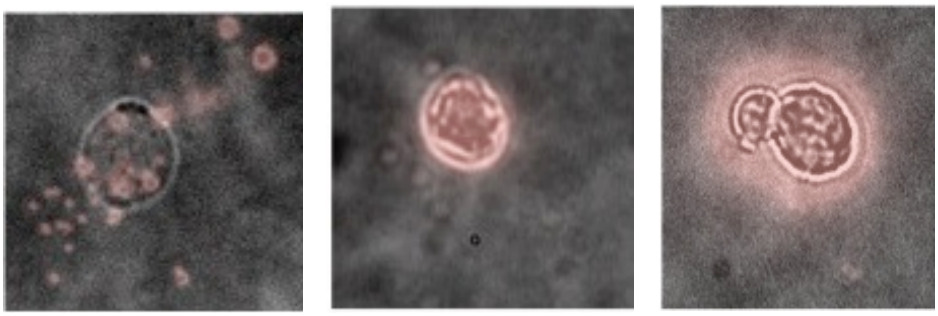

Figure 14 - Cationic GPs Binding Results with 100nm r-PS: *A,* Binding Capacity Graph showing the calculated binding capacity for cationic GPs bound to fluorescent 100nm polystyrene nanoparticles at a ratio of 100 NP/GP. *B,* Fluorescent microscopy images for 100nm r-PS bound to GP, 25k PEI-GP, and Q-GP.

A

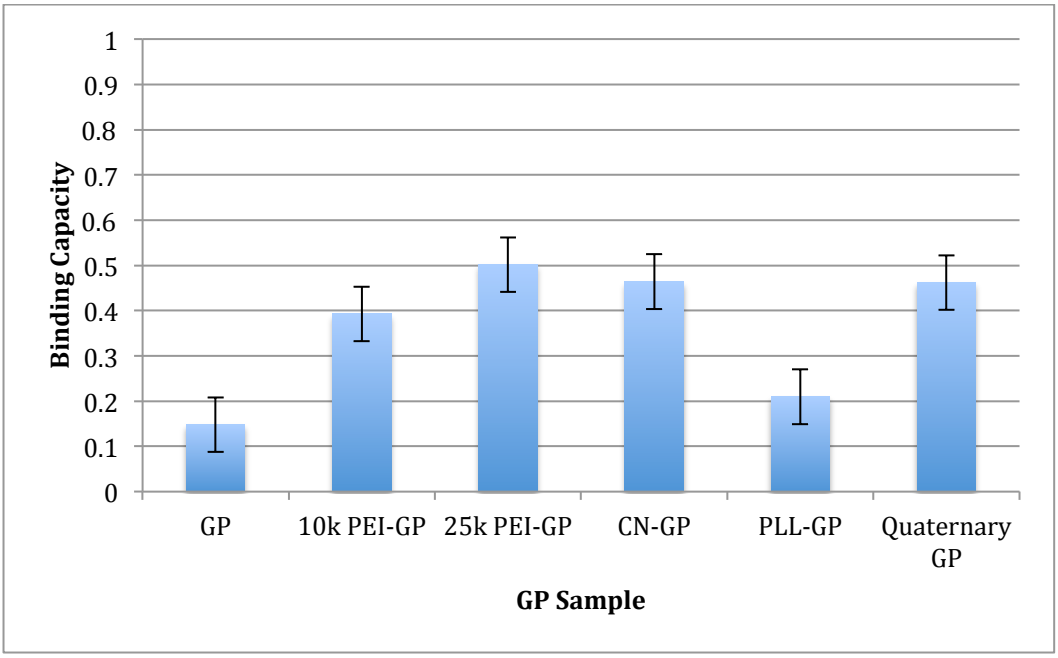

B

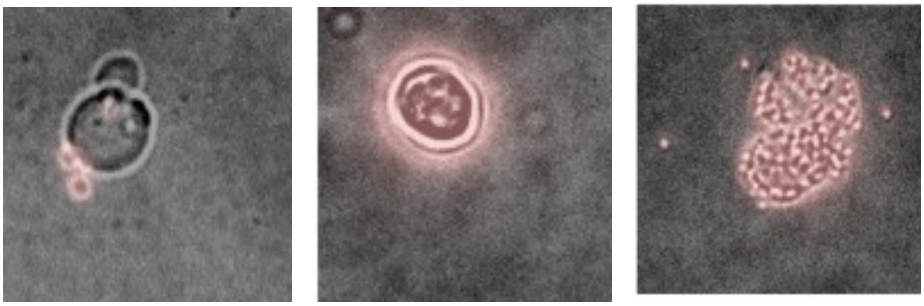

Figure 15 - Cationic GPs Binding Results with 200nm r-PS: *A,* Binding Capacity Graph showing the calculated binding capacity for cationic GPs bound to fluorescent 200nm polystyrene nanoparticles at a ratio of 100 NP/GP. *B,* Fluorescent microscopy images for 200nm r-PS bound to GP, 25k PEI-GP, and Q-GP.

A

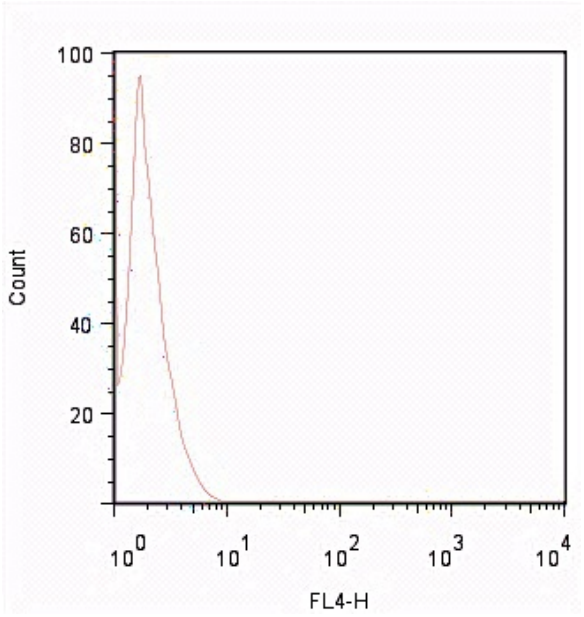

B

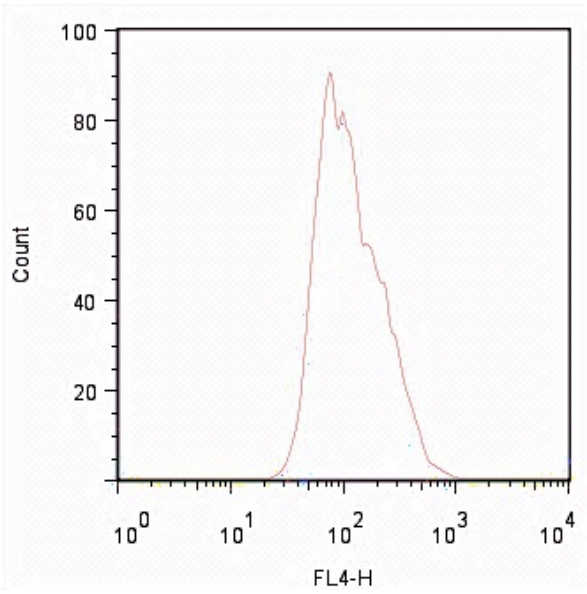

Figure 16 - FACS Results for Cationic GPs with 200nm r-PS: *A,* FACS graph for unmodified GP with 200nm r-PS. *B,* FACS graph for 25k PEI-GP with 200nm r-PS.

A

GP Sample	Zeta Potential Maximum	Zeta Potential Maximum with nanoparticles
GP	-2.09	-1.70
10k PEI-GP	17.6	-13.2
25k PEI-GP	19.2	-24.2
CN-GP	21.0	-24.0
PLL-GP	9.01	-46.6
Q-GP	19.6	-13.6

B

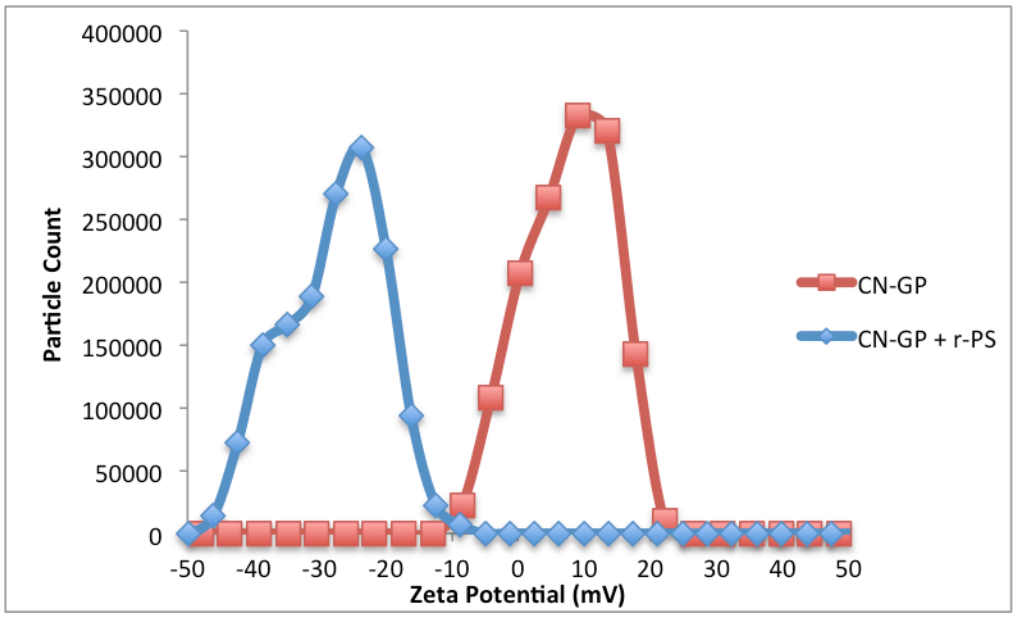

Figure 17 – Zeta Potential Results +/- 200nm r-PS: *A,* Zeta Potential measurements for cationic GPs and cationic GPs bound to 200nm r-PS nanoparticles. *B,* A sample plot of the zeta potential shift of cationic GPs +/- 200nm r-PS.

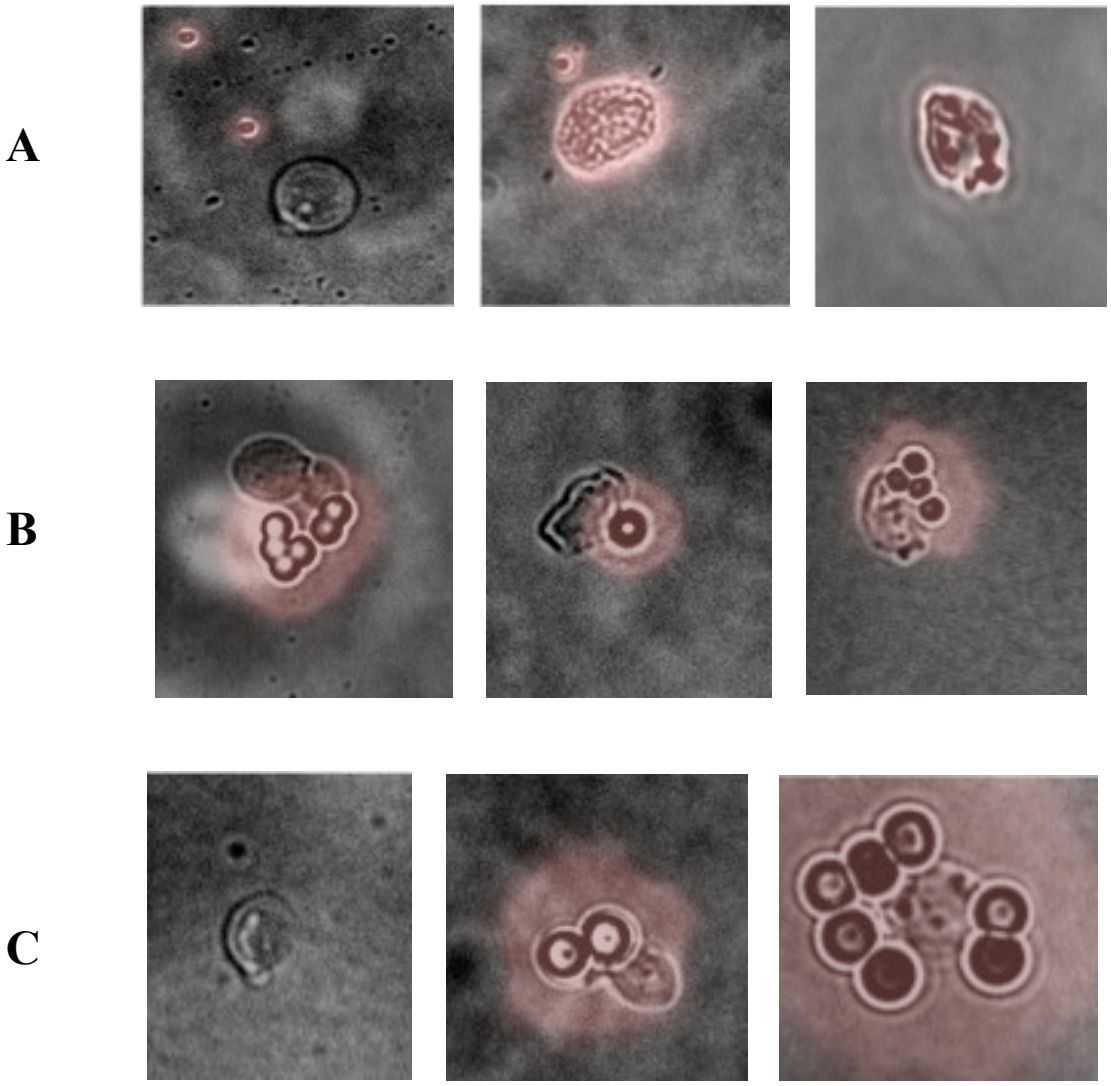

Figure 18 - Cationic GP Binding Results with Larger r-PS Nanoparticles: *A,* GP, 10k PEI-GP, and CN-GP bound to 500nm polystyrene nanoparticles. *B,* GP, 10k PEI-GP, and CN-GP bound to 1µm nanoparticles. *C,* GP, 10k PEI-GP, and CN-GP bound to 2µm nanoparticles.

A

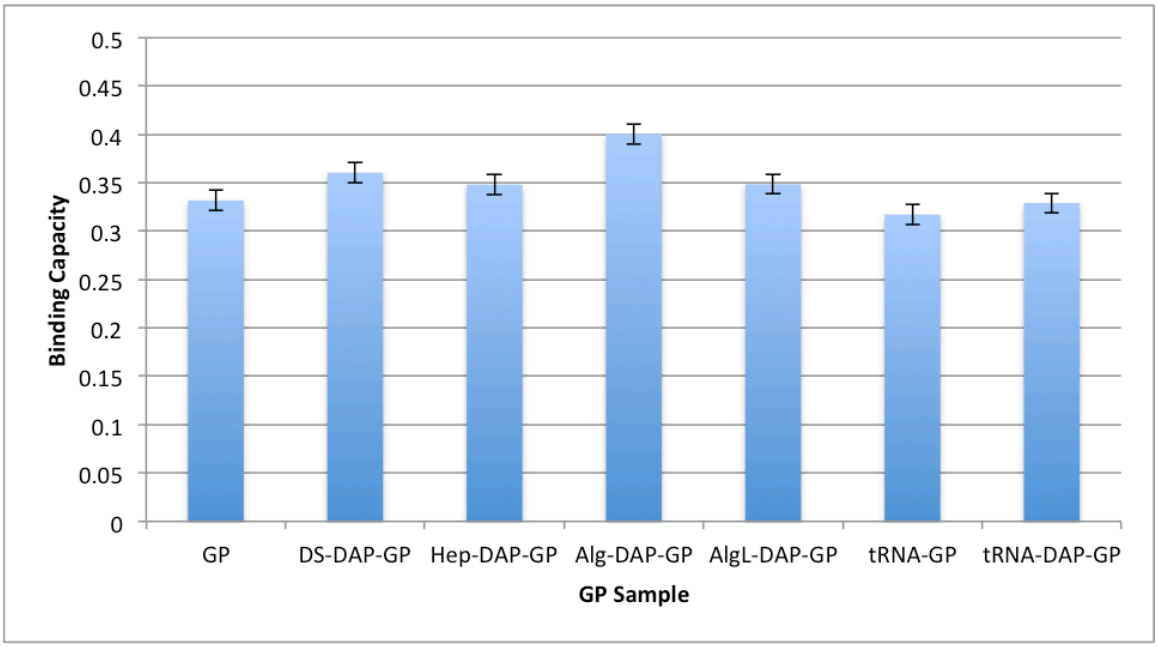

B

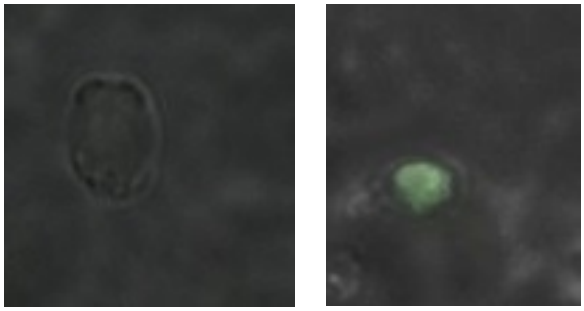

C

GP Sample	Zeta Potential Maximum	Zeta Potenetial Maximum with nanoparticles
GP	-2.09	-8.73
DS-DAP-GP	12.1	-3.70
Hep-DAP-GP	10.0	-0.79
AlgL-DAP-GP	-18.2	-3.32
tRNA-DAP-GP	-16.8	-6.56

Figure 19 - Anionic GP Binding Results with 100nm Latex: *A,* Binding Capacity Graph showing the calculated binding capacity for anionic GPs bound to fluorescent 100nm latex nanoparticles at a ratio of 10 NP/GP. *B,* Fluorescent microscopy images for 200nm r-PS bound to GP and AlgL-DAP-GP. *C,* Zeta Potential measurements for anionic GPs and anionic GPs bound to 100nm latex nanoparticles.

A

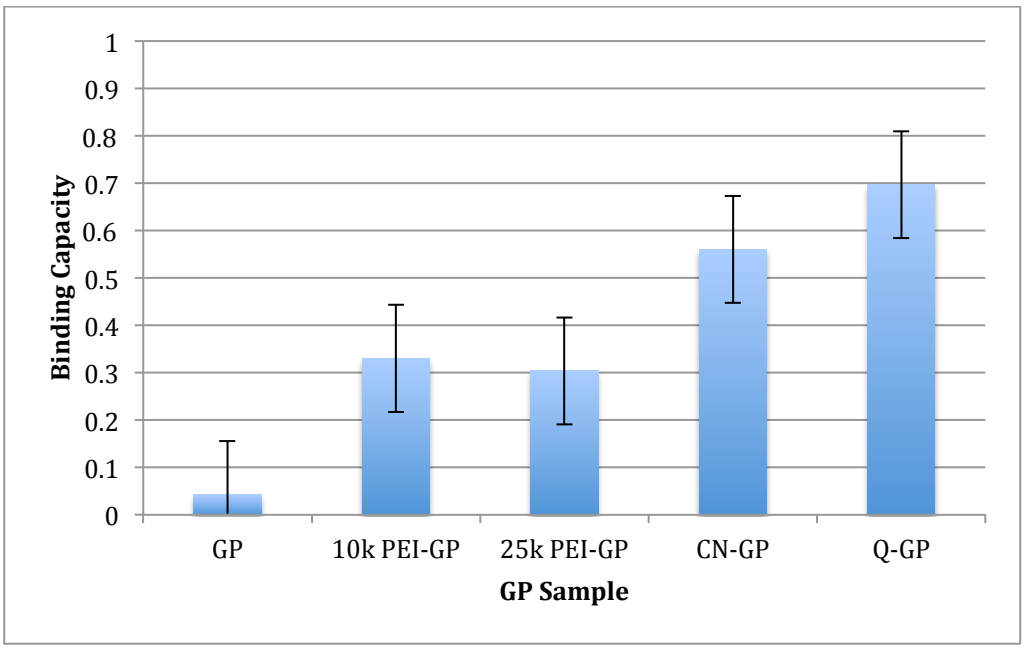

B

C

GP Sample	Zeta Potential Maximum	Zeta Potential Maximum with polymer
GP	-2.09	-8.10
10k PEI-GP	17.6	-22.2
25k PEI-GP	19.2	3.40
CN-GP	21.0	-11.5
Q-GP	19.6	-20.0

Figure 20 - Cationic GP Binding Results with Cy3-siRNA: *A,* Binding Capacity Graph showing the calculated binding capacity for cationic GPs bound to fluorescent Cy3-siRNA. *B,* Fluorescent microscopy images for Cy3-siRNA bound to GP, 25k PEI-GP, and Q-GP. *C,* Zeta Potential measurements for cationic GPs and cationic GPs bound to Cy3-siRNA.

A

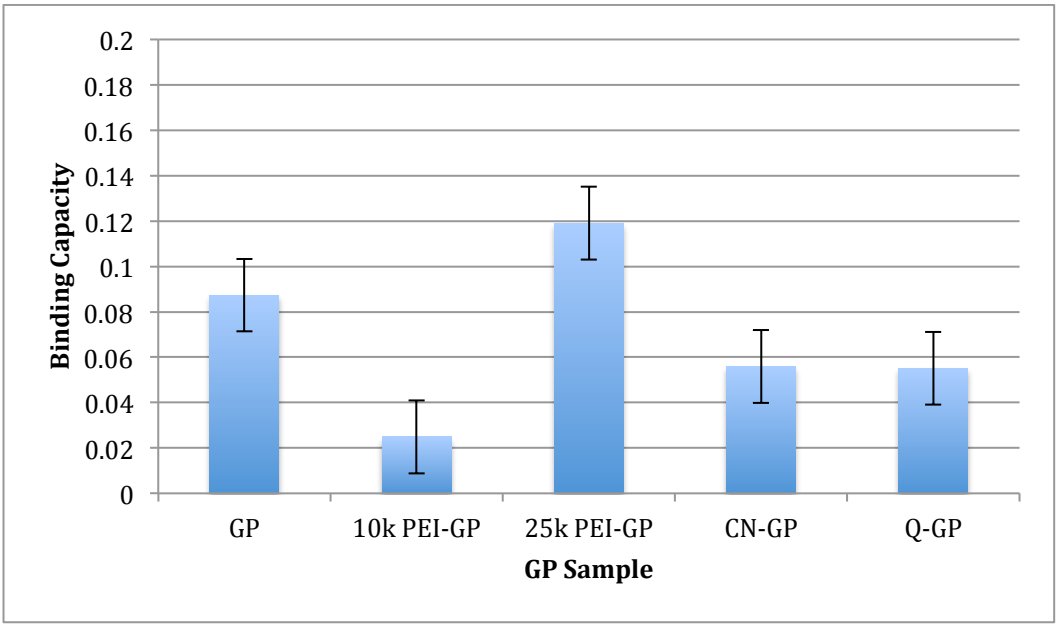

B

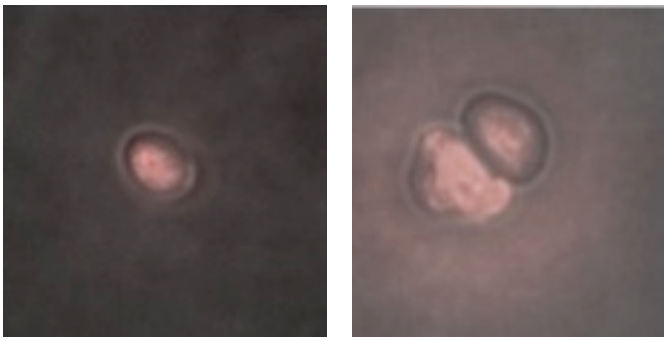

Figure 21 - Cationic GP Binding Results with r-DNA: *A,* Binding Capacity Graph showing the calculated binding capacity for cationic GPs bound to fluorescent r-DNA. *B,* Fluorescent microscopy images for r-DNA bound to GP and 25k PEI-GP.

A

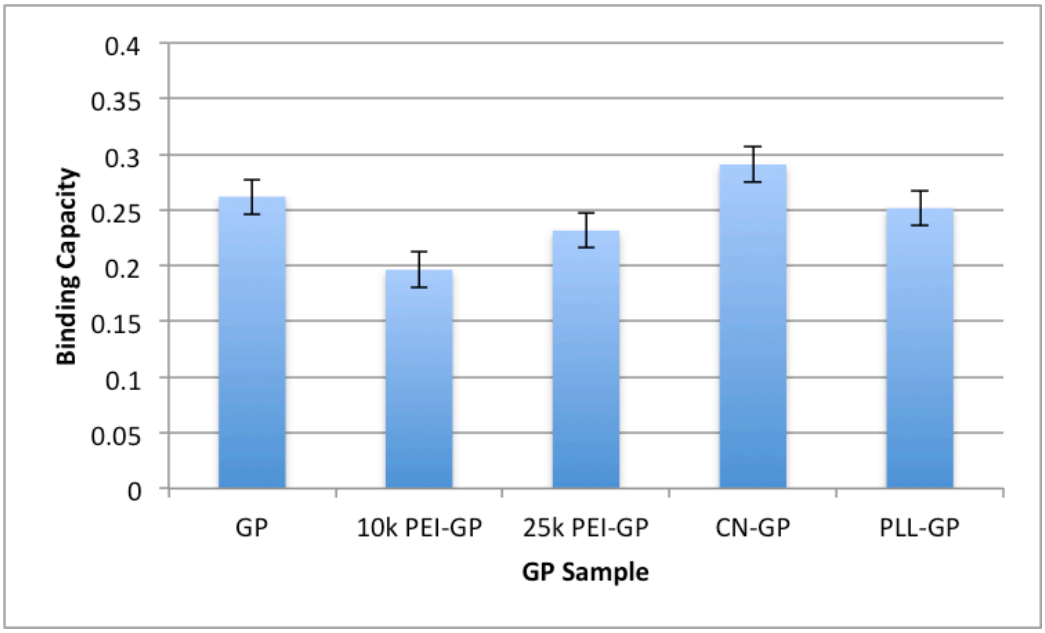

B

Figure 22 - Cationic GP Binding Results with r-tRNA: *A,* Binding Capacity Graph showing the calculated binding capacity for cationic GPs bound to fluorescent r-tRNA. *B,* Fluorescent microscopy images for r-tRNA bound to GP, CN-GP, and Q-GP.

A

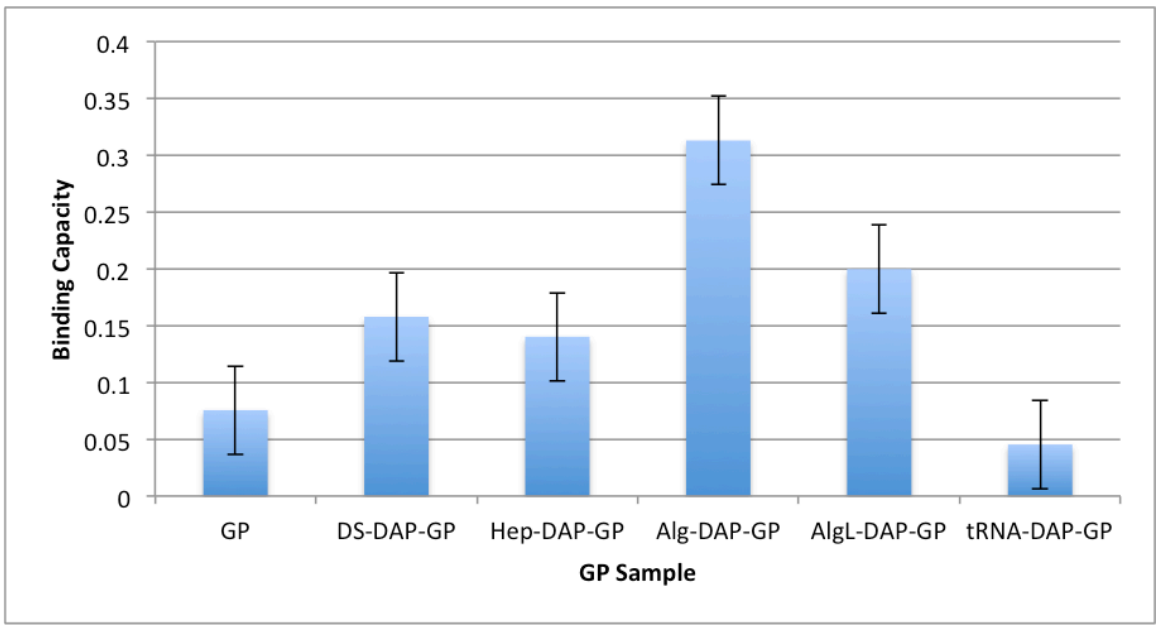

B

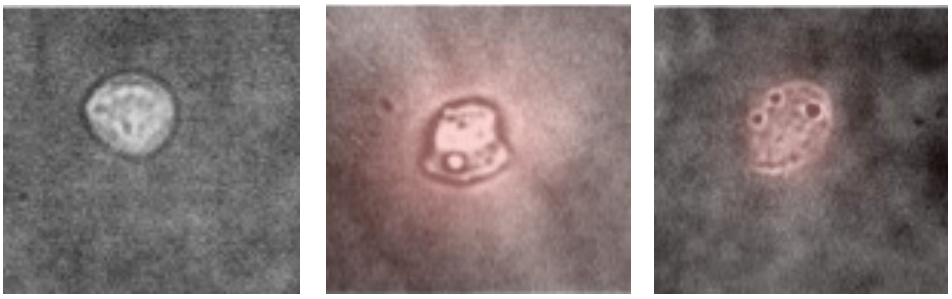

Figure 23 - Anionic GP Binding Results with r-10k PEI: *A,* Binding Capacity Graph showing the calculated binding capacity for anionic GPs bound to fluorescent r-10k PEI. *B,* Fluorescent microscopy images for r-10k PEI bound to GP, Alg-DAP-GP, and AlgL-DAP-GP.

A

GP Sample	Transfection Efficiency (%)
GP	3.5
10k PEI-GP	0.5
25k PEI-GP	3.2
CN-GP	26.2
PLL-GP	4.8
Q-GP	0.3

B

GP Sample	DNA Concentration (μg/1x10^6 particles)	Transfection Efficiency (%)
CN-GP	0.050	25.8
CN-GP	0.125	5.5
CN-GP	0.250	3.8
CN-GP	0.500	1.8

C

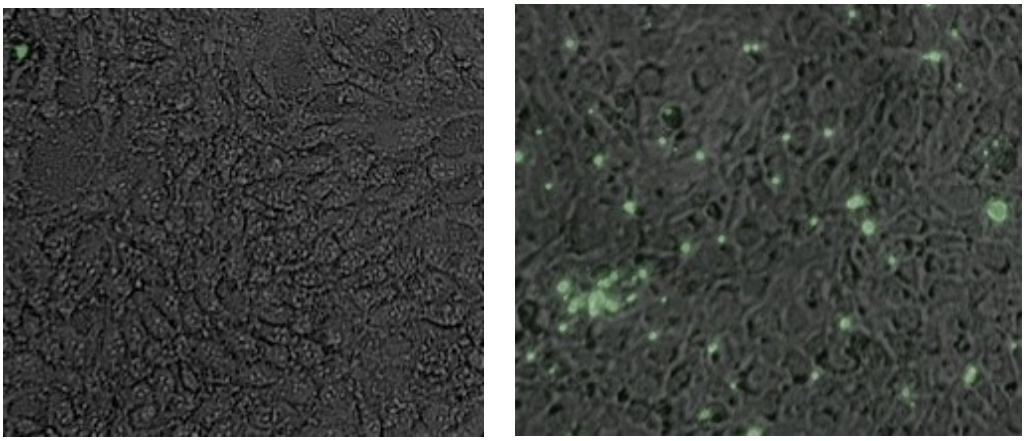

Figure 24 - DNA Transfection Results: *A,* Transfection efficiency of cationic GPs using gWizGFP DNA. *B,* Transfection Efficiency of CN-GP with varying concentrations of gWizGFP DNA. *C,* Fluorescent microscopy images of 3T3-D1 cells transfected by gWizGFP DNA bound to GP and CN-GP.

A

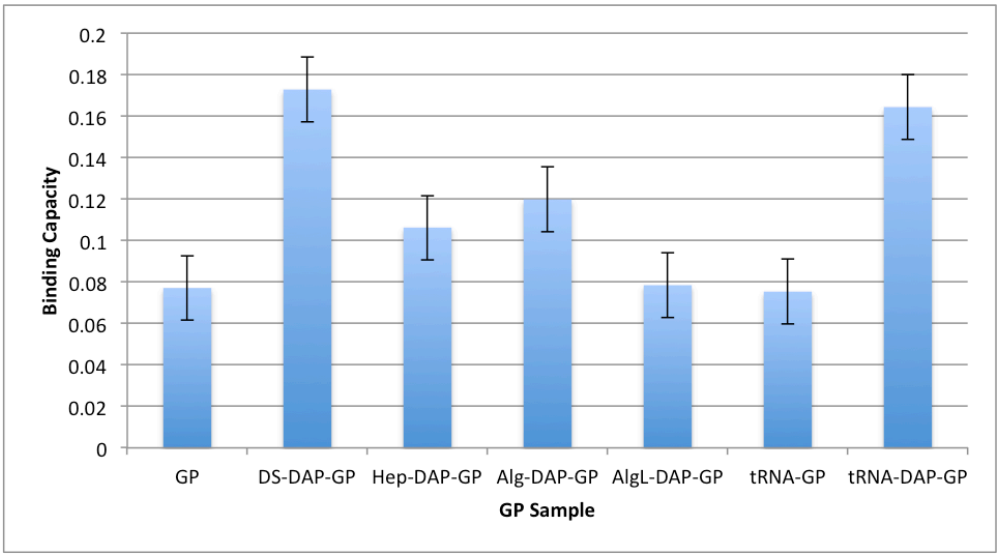

B

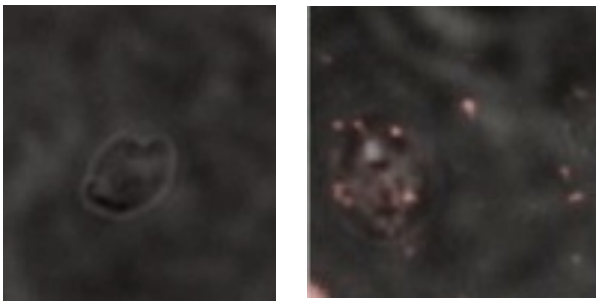

C

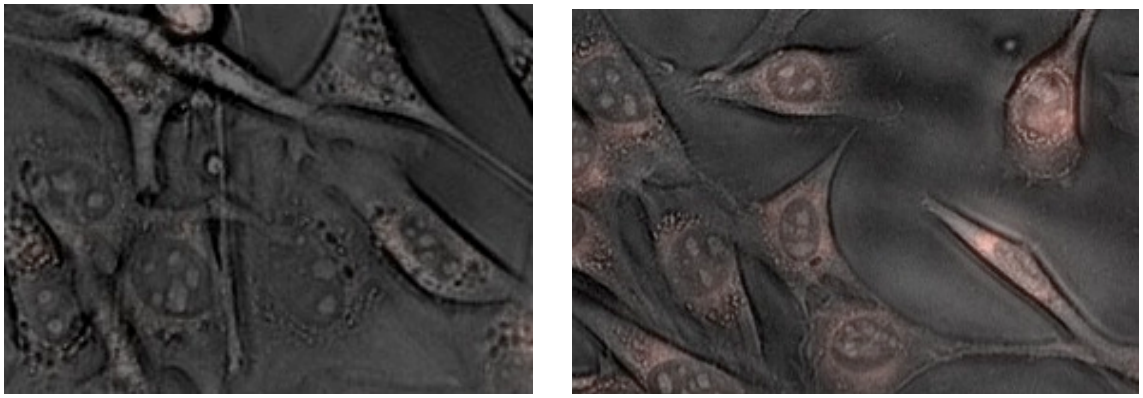

Figure 25 - Dox Binding and Uptake: *A,* Binding Capacity Graph showing the calculated binding capacity for anionic GPs bound to fluorescent Dox. *B,* Fluorescent microscopy images for Dox bound to GP and tRNA-DAP-GP. *C,* Fluorescent microscopy images of 3T3-D1 cells that have taken up Dox bound to GP and tRNA-DAP-GP.

A

B

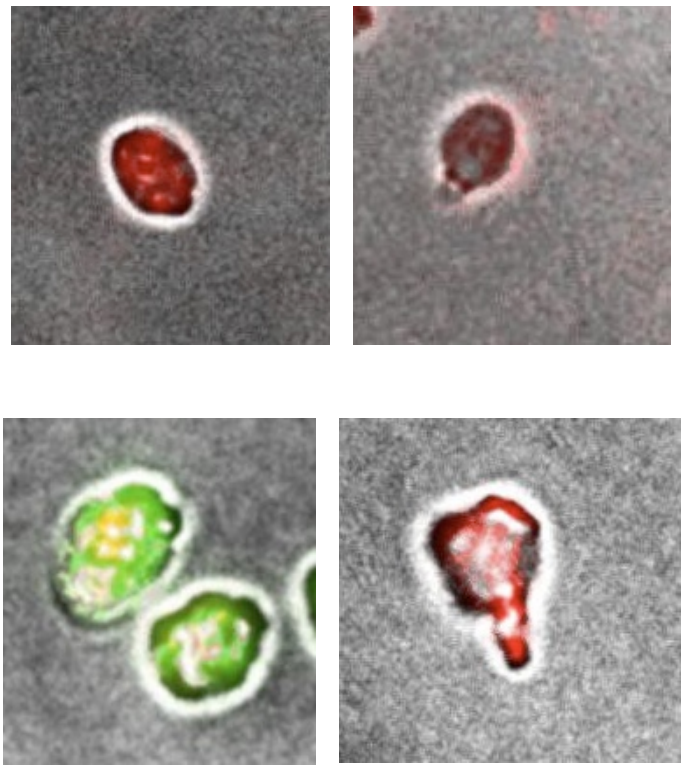

Figure 26 – Click Chemistry Results: *A,* GP and N3-GP after tRNA/PEI core addition. *B,* GP and N3-GP after f-alkyne surface addition.

Bibliography

Adams, D.R; Bhatnagar, S.P. "The Prins Reaction". *Synthesis.* **1977,** 10, 661-672.

Aoudai, M; Tesz, G. J; Nicoloro, S. M; Wang, M; Chouinard, M; Soto, E; Ostroff, G. R; Czech, M. P. "Orally delivered siRNA targeting macrophage MAP4K4 suppresses systematic inflammation". *Nature.* **2009,** 458, 1180-1184.

Azzam, T; Eliyahu, H; Shapira, L; Linial, M; Barenholz, Y; Domb, A.J. "Polysaccharide-Oligoamine Based Conjugates for Gene Delivery". *Journal of Medicinal Chemistry.* **2002,** 45, 1817-1824.

Bertschinger, M; Chaboche, S; Jordan, M; Wurm, F.M. "A spectrophotometric assay for the quantification of polyethyleneimine in DNA nanoparticles". *Analytical Biochemistry.* **2004,** 334, 196-198.

Brown, G.D; Gordon, S. "Immune recognition: a new receptor for β-glucans". *Nature.* **2001**, 413, 36-37.

Friedman, M. "Applications of the Ninhydrin Reaction for Analysis of Amino Acids, Peptides, and Proteins to Agricultural and Biomedical Sciences". *Journal of Agricultural and Food Chemistry.* **2004,** 52, 385-406.

Helms, B; Mynar, J.L; Hawker, C.J; Fréchet, J.M.J. "Dendronized Polymers via 'Click Chemistry'". *Journal of the American Chemical Society.* **2004,** 126, 15020-15021.

Kolb, H. C; Finn, M. G; Sharpless, K. B. "Click Chemistry: Diverse Chemical Function from a Few Good Reactions". *Angew. Chem. Int. Ed.* **2001,** 40, 2004-2021.

Li, C. "Organic Reactions in Aqueous Media with a Focus on Carbon-Carbon Bond Formations: A Decade Update". *Chemical Review.* **2005,** 105, 3095-3165.

Pastor, I.M; Yus, M. "The Prins Reaction: Advances and Applications". *Current Organic Chemistry.* **2007,** 11, 925-957.

Soto, E. R; Ostroff, G.R. "Characterization of Multilayered Nanoparticles Encapsulated in Yeast Cell Wall Particles for DNA Delivery." *Bioconjugate Chemistry.* **2008,** 19, 840-848.

Soto, E; Ostroff, G. "Glucan Particles as an efficient siRNA delivery vehicle". *NSTI Nanotech 2008 Technical Proceedings Volume 2.* **2008,** 332-335.

Soto, E; Kim, Y.S; Lee, J; Kornfeld, H; Ostroff, G. "Glucan Particle Encapsulated Rifampicin for Targeted Delivery of Macrophages". *Polymers.* **2010,** 2, 681-689.

Soto, E; Ostroff, G. "Use of β-Glucans for Drug Delivery Applications" Chapter 5, 48-67. In "Biology and Chemistry of Beta Glucan, Volume 1: Beta Glucans - Mechanisms of Action". V. Vetvicka and M. Novak (Eds). 2011, Bentham Press, 82 pp. In press.

Tesz, G. J; Aouadi, M; Prot, M; Nicoloro, S. M; Boutet, E; Amano, S. U; Goller, A; Wang, M; Guo, C; Salomon, W. E; Virbasius, J. V; Baum, R. A; O'Connor Jr, M. J; Soto, E; Ostroff, G. R; Czech, M. P. "Glucan Particles for Selective Delivery of siRNA to Phagocytic Cells in Mice". *Biochemical Journal*. 2011, In press.

Thielbeer, F; Donaldson, K; Bradley, M. "Zeta Potential Mediated Reaction Monitoring on Nano and Microparticles". *Bioconjugate Chemistry.* **2011,** 22, 144-150.

Wu, J; Su, Z; Ma, G. "A thermo- and pH-sensitive hydrogel composed of quaternary chitosan/glycerophosphate". *International Journal of Pharmaceutics.* **2006,** 315, 1-11.

Wei, W; Ma, G; Wang, L; Wu, J; Su, Z. "Hollow quaternized chitosan microspheres increase the therapeutic effect of orally administered insulin". *Acta Biomaterialia.* **2010,** 6, 205-209.

[i] Brown, G.D; Gordon, S. "Immune recognition: a new receptor for β-glucans". *Nature.* **2001**, 413, 36-37.
[ii] Soto, E. R; Ostroff, G.R. "Characterization of Multilayered Nanoparticles Encapsulated in Yeast Cell Wall Particles for DNA Delivery." *Bioconjugate Chemistry* **2008,** 19, 840-848.
[iii] Soto, E. R; Ostroff, G.R. "Characterization of Multilayered Nanoparticles Encapsulated in Yeast Cell Wall Particles for DNA Delivery." *Bioconjugate Chemistry* **2008,** 19, 840-848.
[iv] Soto, E; Ostroff, G. "Glucan Particles as an efficient siRNA delivery vehicle". *NSTI Nanotech 2008 Technical Proceedings Volume 2.* **2008,** 332-335.
[v] Aoudai, M; Tesz, G. J; Nicoloro, S. M; Wang, M; Chouinard, M; Soto, E; Ostroff, G. R; Czech, M. P. "Orally delivered siRNA targeting macrophage MAP4K4 suppresses systematic inflammation". *Nature.* **2009,** 458, 1180-1184.
[vi] Tesz, G. J.; Aouadi, M.; Prot, M.; Nicoloro, S. M; Boutet, E; Amano, S. U; Goller, A; Wang, M; Guo, C; Salomon, W. E; Virbasius, J. V; Baum, R. A; O'Connor Jr, M. J; Soto, E; Ostroff, G. R; Czech, M. P. "Glucan Particles for Selective Delivery of siRNA to Phagocytic Cells in Mice". *Biochemical Journal*. 2011, In press.
[vii] Azzam, T; Eliyahu, H; Shapira, L; Linial, M; Barenholz, Y; Domb, A.J. "Polysaccharide-Oligoamine Based Conjugates for Gene Delivery". *Journal of Medicinal Chemistry.* **2002,** 45, 1817-1824.
[viii] Kolb, H. C; Finn, M. G; Sharpless, K. B. "Click Chemistry: Diverse Chemical Function from a Few Good Reactions". *Angew. Chem. Int. Ed.* **2001,** 40, 2004-2021.
[ix] Soto, E; Ostroff, G. "Use of β-Glucans for Drug Delivery Applications" Chapter 5, 48-67. In "Biology and Chemistry of Beta Glucan, Volume 1: Beta Glucans - Mechanisms of Action". V. Vetvicka and M. Novak (Eds). 2011, Bentham Press, 82 pp. In press.
[x] Wu, J; Su, Z; Ma, G. "A thermo- and pH-sensitive hydrogel composed of quaternary chitosan/glycerophosphate". *International Journal of Pharmaceutics.* **2006,** 315, 1-11.
[xi] Wei, W; Ma, G; Wang, L; Wu, J; Su, Z. "Hollow quaternized chitosan microspheres increase the therapeutic effect of orally administered insulin". *Acta Biomaterialia.* **2010,** 6, 205-209.
[xii] Soto, E. R; Ostroff, G.R. "Characterization of Multilayered Nanoparticles Encapsulated in Yeast Cell Wall Particles for DNA Delivery." *Bioconjugate Chemistry* **2008,** 19, 840-848.
[xiii] Friedman, M. "Applications of the Ninhydrin Reaction for Analysis of Amino Acids, Peptides, and Proteins to Agricultural and Biomedical Sciences". *Journal of Agricultural and Food Chemistry.* **2004,** 52, 385-406.